Available online at www.sciencedirect.com
ScienceDirect
Coordination Chemistry Reviews 251 (2007) 610–641
COORDINATION CHEMISTRY REVIEWS
www.elsevier.com/locate/ccr

Review

Metal complexes with 'pincer'-type ligands incorporating *N*-heterocyclic carbene functionalities

David Pugh, Andreas A. Danopoulos *

School of Chemistry, University of Southampton, Highfield, Southampton SOU IBJ, UK

Received 1 May 2006; accepted 3 August 2006
Available online 8 August 2006

Contents

Abstract

The coordination and organometallic chemistry of linear, rigid, tridentate ligands, which incorporate at least one *N*-heterocyclic carbene and other 'classical' donors, is reviewed across the periodic table with emphasis on unique features due to the presence of the *N*-heterocyclic carbene donor.

Keywords: Carbenes; Pincer; Tridentate; Rigid; Crystal structures; Transition metals

Abbreviations: Bu, butyl; Bz, benzyl; COD, 1,5-cyclooctadiene; DBA, dibenzylidene acetone; DCM, dichloromethane; D*i*PP, di*iso*propylphenyl; DMAc, *N*,*N*-dimethylacetamide; DME, 1,2-dimethoxyethane; DMF, *N*,*N*-dimethylformamide; DMS, dimethylsulfide; Et, ethyl; HMDS, hexamethyldisilazide; Me, methyl; Mes, mesityl(2,4,6-trimethylphenyl); Nbd, norbornadiene; NHC, *N*-heterocyclic carbene; NMO, *N*-methylmorpholine-*N*-oxide; NMR, nuclear magnetic resonance; OAc, acetate; OTf, trifluoromethanesulfonate; Ph, phenyl; ppm, parts per million; Pr, propyl; py, pyridine; RT, room temperature; TEA, triethylamine; TMS, trimethylsilyl; TON, turnover number; Xy, Xylyl(2,6-dimethylphenyl); tmeda, *N*,*N*,*N*′,*N*′-tetramethylethylene diamine

* Corresponding author.
E-mail address: adl@soton.ac.uk (A.A. Danopoulos).

0010-8545/$ – see front matter © 2006 Elsevier B.V. All rights reserved.
doi:10.1016/j.ccr.2006.08.001

1. Introduction

The isolation of thermally stable *N*-heterocyclic carbenes by Arduengo in 1991 initiated intense research activity into the organometallic chemistry of these versatile ligands. Furthermore, the ease of functionalisation of the imidazolium salt proligands led to the incorporation of *N*-heterocyclic carbene donors in polydentate ligand structures, usually in combination with other classical donors. The aim of this approach has been the development of functional complexes and the precise tailoring of the metal coordination sphere since dissociation–association reactions, which are important for the generation of active species in homogeneous catalysis, are not possible in the kinetically formed NHC complexes due to the strength of the metal–NHC bonding [1]. The first classical donor functionalised *N*-heterocyclic carbene complexes were described by Lappert and comprised saturated imidazolin-2-ylidene donor groups linked to alkenes or phosphines by C3 linkers [2]. The complexation reactions involved cleavage of electron rich olefins by low oxidation state transition metals. The introduction of the silver transmetallation route [3] and the 'bottleable' functionalised *N*-heterocyclic carbenes [4–6] opened up further possibilities for the synthesis of well defined functionalised carbene complexes. Among the polydentate ligand structures with carbene donors, tripodal [7,8] and 'pincer' systems [9–11] have attracted a lot of attention. The rigid linear tridentate and 'pincer' ligands support meridional (in octahedral geometries) or pseudo-meridional (in trigonal bipyramidal, square pyramidal or square planar geometries) coordination. Seminal work with 'pincer' ligands bearing phosphine and amine donors was carried out by Shaw, van der Boom and Milstein [12], Albrecht and van Koten [13] and others. Linear rigid tridentate ligands are being investigated by various groups with metals from across the periodic table [14,15]. In this paper, we review the use of rigid linear tridentate ligands with at least one *N*-heterocyclic carbene donor as shown schematically below (Fig. 1).

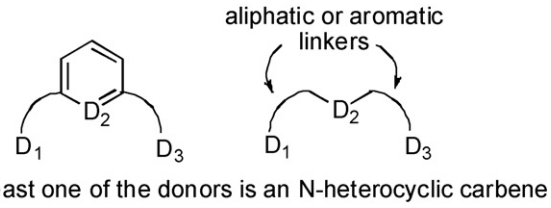

Fig. 1. Generic structures of the ligands featured in this review.

In most cases the above ligands adopt meridional coordination modes with the majority of the transition metals, except group 11 metals. However, complexes with less rigid, long aliphatic linkers may adopt distorted facial coordination modes and therefore have been excluded from this review. A list of the ligand structures discussed is shown below (Fig. 2).

Substantial work with preorganised rigid tridentate ligands incorporating non-cyclic carbene donors of P-heteroatom stabilized carbenes has been described by Cavell, recently reviewed [16,17] and will not be covered any further here. The literature has been covered systematically until March 2006.

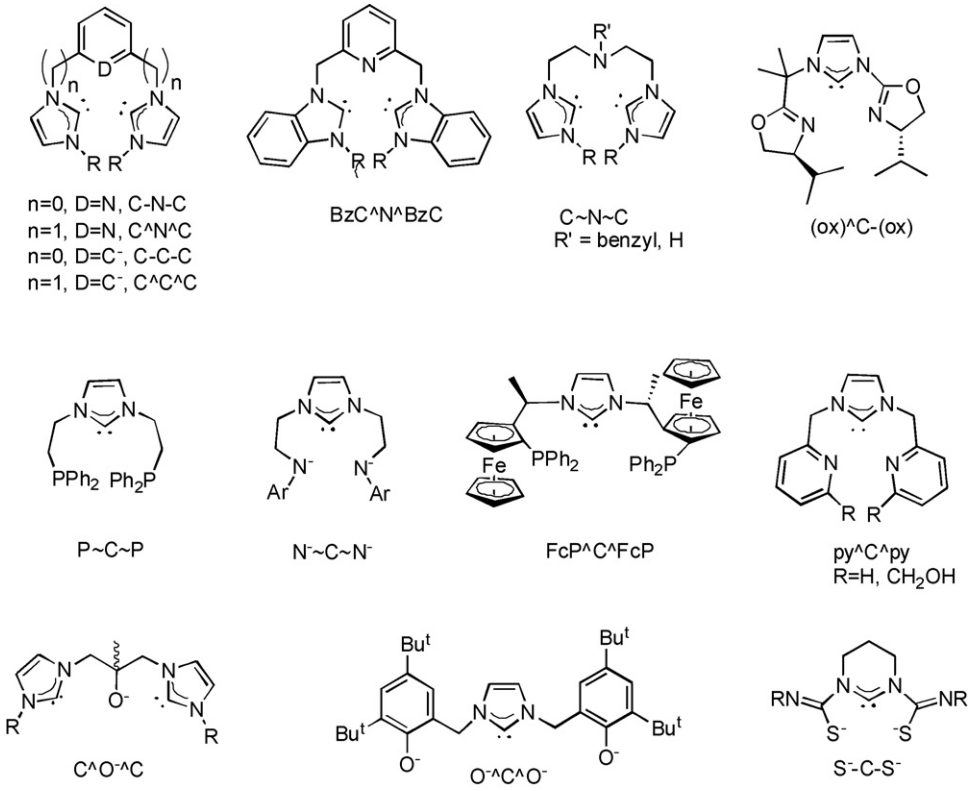

Fig. 2. Structures of the ligands discussed in this review.

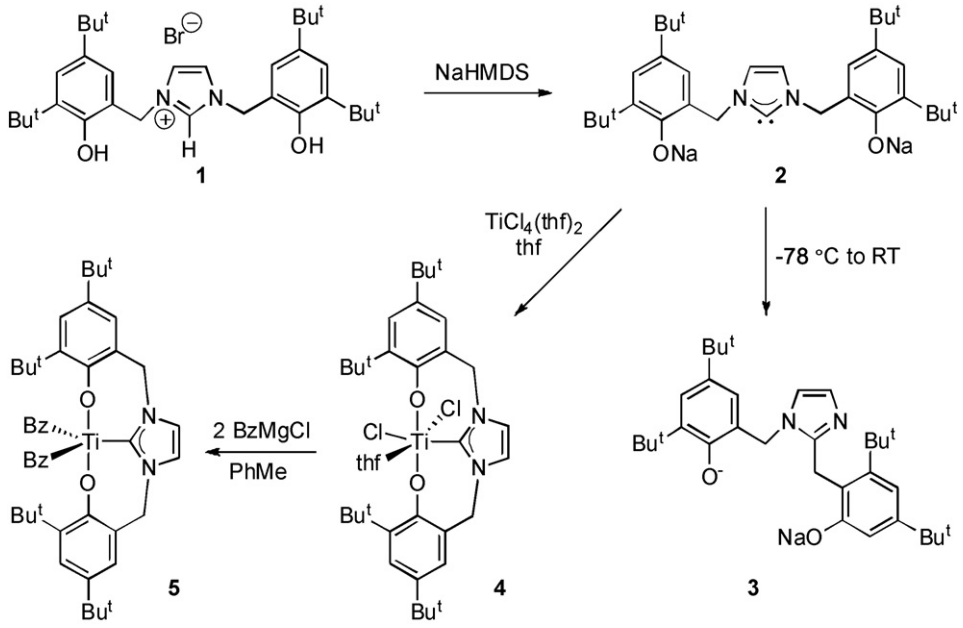

Scheme 1. Synthesis of $(O^{-}–C–O^{-})TiCl_2(thf)$ and $(O^{-}–C–O^{-})TiCl_2(Bz)_2$.

2. Groups 4–7 metal complexes

Examples of early transition metal complexes with rigid tridentate and pincer ligands incorporating one or more NHCs are sparse. An analogous situation prevails with other NHC complexes of the early transition metals.

We have organised the description of these complexes into two sections: the first dealing with monocarbene ligands of the type DCD (D = functional group with anionic N or O atoms; C = NHC), the second with dicarbene complexes of the type CDC (D = functional group with neutral or anionic N or C atoms; C = NHC).

2.1. DCD ligands

The first NHC pincer ligand complexed to an early transition metal appeared in 2003, when Kawaguchi reported the synthesis of an imidazolium-linked bis(phenol) proligand **1** and its Ti(IV) complexes [18]. The proligand was synthesised through successive alkylations on the N atoms of imidazole using 2-bromomethyl-4,6-di-*tert*-butylphenol at 80 °C.

Deprotonation of **1** with 3 equiv. of NaHMDS at −78 °C resulted in the formation of the disodium salt **2**. Upon warming to RT, **2** decomposed *via* a 1,2-benzyl migration to the 2-alkylimidazole derivative **3**. 1,2-Benzyl migration had been noted before with singlet carbenes [19], but migration in **2** was suppressed at low temperatures. Reaction of a thf solution of **2** with $TiCl_4(thf)_2$ at −78 °C resulted in the formation of **4**, $(O^{-}–C–O^{-})TiCl_2(thf)$. This was alkylated with BzMgCl to form the dibenzyl Ti(IV) complex **5**, $(O^{-}–C–O^{-})TiBz_2$ (Scheme 1).

Single crystal X-ray diffraction studies were carried out on both **4** and **5** (Fig. 3). Complex **4** is a monomeric six coordinate octahedral species with *cis* chloride ions and coordinating thf. Complex **5** is a five coordinate species, whose geometry is best described as distorted trigonal bipyramidal. The 'degree of trigonality', τ [20], is calculated to be 0.66 (0 = ideal square-based pyramidal; 1 = ideal trigonal bipyramidal), indicating substantial distortion of the trigonal bipyramidal geometry.

The Ti–C_{NHC} distances of 2.200(9) Å (**4**) and 2.187(3) Å (**5**) are identical within experimental error and are within the range reported for other known Ti(IV)–C_{NHC} bonds (2.194(7)–2.313(5) Å) [21,22]. The $^{13}C\{^{1}H\}$ NMR signal for the C_{NHC} in **5** was observed at 188.3 ppm which is substantially deshielded relative to the C_{NHC} in **4** (164.0 ppm). Caution, however, should be exercised in the assignment of the C_{NHC} signal in the $^{13}C\{^{1}H\}$ NMR spectra, which sometimes is not observed [22]. This has led to erroneous assignment of deshielded aromatic signals as C_{NHC}.

Fryzuk reported the synthesis of the bis(amido)carbene zirconium complex **8** from the reaction of ligand **7** with $Zr(NEt_2)_4$ (Scheme 2) [23]. Complex **7** was synthesised by reduction of

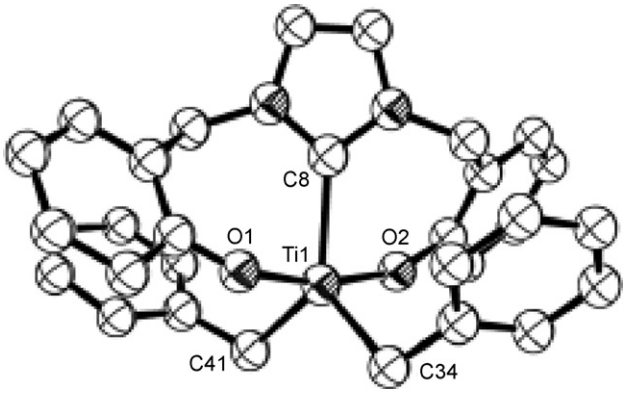

Fig. 3. X-ray structure of **5**; ^{t}Bu groups omitted for clarity [18].

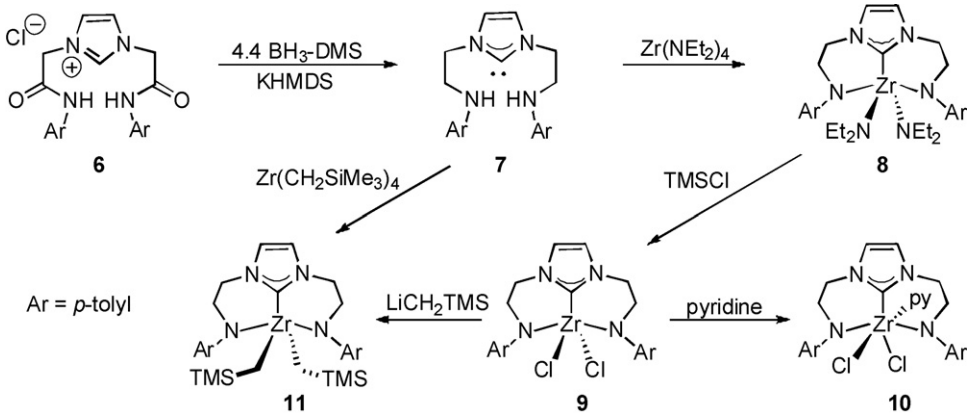

Scheme 2. Synthesis of bisamido carbene complexes of zirconium.

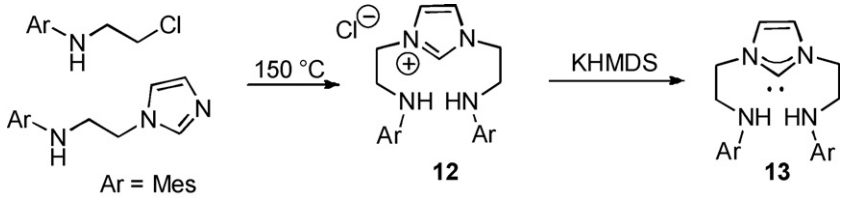

Scheme 3. Synthesis of bisamine carbenes with bulky aromatic substituents at N.

the corresponding bis(amide)imidazolium salt with excess BH_3, followed by deprotonation with KHMDS.

Organic amides with bulkier aromatic groups (Ar = mesityl, 2,6-D*i*PP) led to decomposition during the borane reduction step. However, melting of the appropriate β-chloroethylaniline with a suitably substituted imidazole at 150 °C led to the bis(amine)imidazolium salt **12**. Deprotonation of **12** with KHMDS yielded the bis(amine)carbene ligand **13** (Scheme 3) [24].

Reaction with TMSCl led to substitution of the NEt_2 groups in **8** by chloride ions. Alkylation with $TMSCH_2Li$ (Scheme 4) afforded dialkyl complexes which were also obtained by the reaction of $Zr(CH_2TMS)_4$ with carbene **7**. X-ray crystallographic analysis of $^{tol}(N^-{\sim}C{\sim}N^-)ZrCl_2$(pyridine) (**10**) and $^{tol}(N^-{\sim}C{\sim}N^-)Zr(CH_2TMS)_2$ (**11**, Fig. 4) was carried out.

Complex **10** is a six coordinate octahedral species with *cis* chloride ions, similar to the structure of **4** where the solvating ligand is not *trans* to the carbene. Complex **11** is a five coordinate species described as distorted trigonal bipyramidal, although the τ value of 0.20 suggests distorted square-based pyramidal would be a more accurate description. The Zr–C_{NHC} distances of 2.391(5) Å (**10**) and 2.415(3) Å (**11**) are within the range of known Zr(IV)–C_{NHC} bonds (2.299(1)–2.456(3) Å) [25,26]. The $^{13}C\{^1H\}$ NMR signals for the C_{NHC} were seen at 188.8 ppm (**8**), 181.0 ppm (**10**) and 186.8 ppm (**11**).

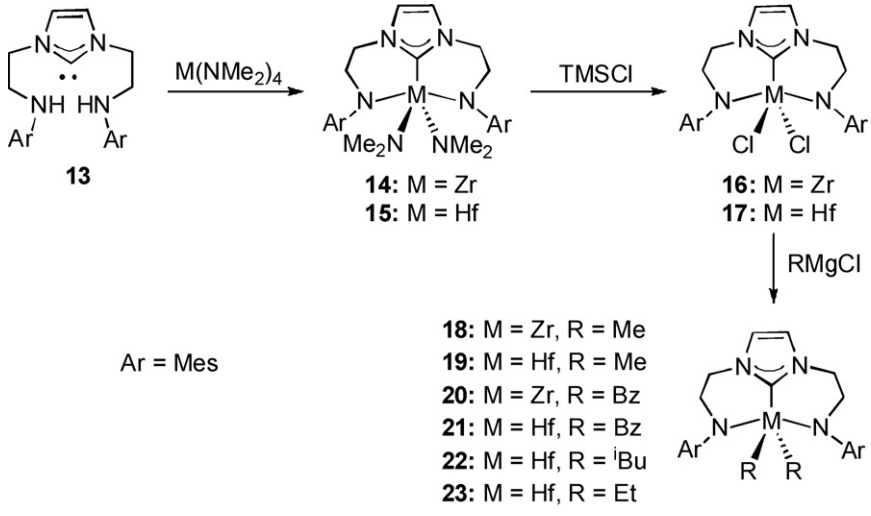

Scheme 4. Synthesis of $(N^-{\sim}C{\sim}N^-)$Hf alkyl complexes.

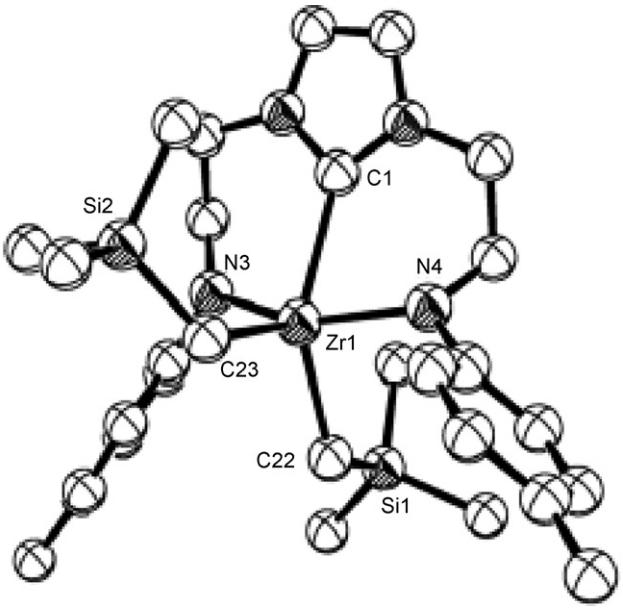

Fig. 4. X-ray structure of **11** [23].

Reaction of **13** with $Zr(NMe_2)_4$ and $Hf(NMe_2)_4$ afforded the zirconium and hafnium complexes $^{mes}(N^-\sim C\sim N^-)Zr(NMe_2)_2$ (**14**) and $^{mes}(N^-\sim C\sim N^-)Hf(NMe_2)_2$ (**15**), respectively. These were converted to $^{mes}(N^-\sim C\sim N^-)ZrCl_2$ (**16**) and $^{mes}(N^-\sim C\sim N^-)HfCl_2$ (**17**) by the reaction with TMSCl. Alkylation of **16** with MeMgCl and BzMgCl produced zirconium dialkyl complexes **18** and **20**, respectively. Alkylation of **17** with MeMgCl, BzMgCl, ^{i}BuMgCl and EtMgCl produced the corresponding hafnium dialkyl complexes **19**, **21**–**23** (Scheme 4).

The C_{NHC} signals in the $^{13}C\{^1H\}$ NMR spectra were seen at 190.9 ppm (**14**), 192.3 ppm (**16**), 189.8 ppm (**18**) and 190.1 ppm (**20**). All the complexes **14**–**23** are five coordinate, although the only X-ray diffraction study was reported for **22** (Fig. 5). It is described as distorted trigonal bipyramidal, with a τ value of 0.29 indicating substantial distortion. The Hf–C_{NHC} bond length of 2.385(3) Å is slightly shorter than other known Hf(IV)–C_{NHC} bond lengths (2.401(2)–2.406(6) Å) [26,27].

The hafnium diethyl complex **23** is thermally unstable, decomposing at RT by means of β-hydrogen elimination to give ethane and a hafnium η^2-ethylene complex. The ethylene complex immediately underwent C–H activation on one of the *o*-methyl groups on the mesityl group. Attempts to trap the ethylene complex with pyridine and PMe_3 were unsuccessful.

Addition of 2 equiv. of isopropyl isocyanide to the hafnium complex **19** resulted in the formation of **24**, where both isocyanide groups have inserted into Hf–Me bonds to form an iminoacyl complex. The mono-insertion product **25** was formed by the reaction of **19** with 1 equiv. of isocyanide. Further reaction with isocyanide afforded bis-insertion products (**26**, **27**). Reaction with CO gave an eneamidolate metallacycle **28** (Scheme 5).

Structural characterisation of **25**, **26** and **28** revealed that the tridentate ligand became substantially distorted away from meridionally into a facially capping coordinating mode, possibly due to the flexibility of the ligand system. Departure from the meridional coordination mode was also observed in the five coordinate complexes **11** and **22**, although to a lesser extent; the distance of the metal from the plane defined by the three donor atoms of the ligand did not exceed 0.439 Å (**22**). In contrast, the analogous distance of the Hf atom in **25**, **26** and **28**, was at least 0.813 Å (**25**). Based on these metrical data, we considered **11** and **22** as rigid tridentate 'pincer' complexes with a distorted meridional ligand, whereas in **25**, **26** and **28** the ligands adopt a facially capping geometry.

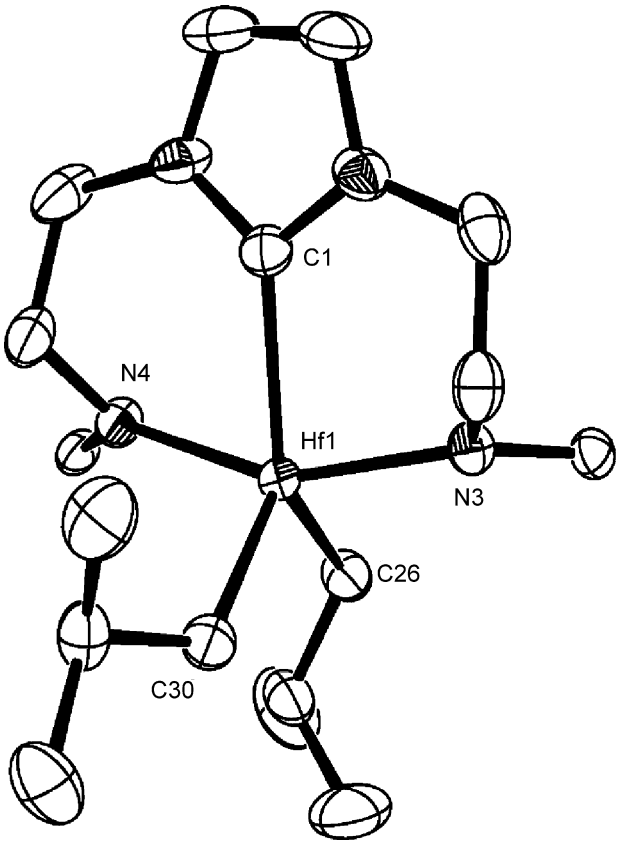

Fig. 5. X-ray structure of **22**; Mes groups bar *ipso* carbons omitted for clarity [24].

Reaction of the hafnium dimethyl complex **19** with CO (1 bar) gave the hafnium vinylenolate complex **31** (Scheme 6). Monitoring of the reaction by $^{13}C\{^1H\}$ NMR spectroscopy showed the presence of a signal at 339.6 ppm which was assigned to the acyl carbon of Hf(η^2-acyl) complexes. Rearrangement of the acyl complex **29** to the vinylenolate **31** is thought to occur *via* a hydrogen shift from the methyl group to the acyl carbon.

The reactivity of the ^{iso}butyl hafnium complex **22** towards CO proceeds along the same initial pathway: insertion of CO into the Hf–C bond, as noted by a ^{13}C NMR signal at 338.4 ppm. However, hydrogen migration to form the vinylenolate does not occur; instead, a second CO insertion takes place and a dihafnium bis(enediolate) complex, **33**, is formed. It was suggested that the mononuclear hafnium enediolate **32** is formed after the second CO insertion, which then dimerises to form the 10-membered dihafnium macrocycle (Scheme 6).

Single crystal diffraction studies of **33** were carried out, revealing again a facially capping coordination mode of the ligand.

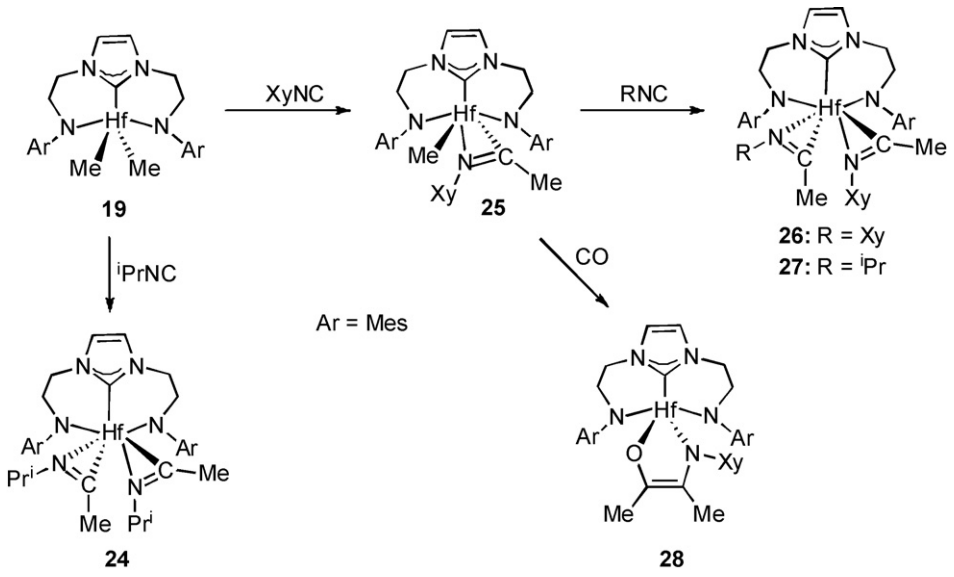

Scheme 5. Reactivity of the hafnium dialkyl complex **19**.

2.2. CDC ligands

The first report of a chromium C–N–C 'pincer' complex appeared in 2003 [28]. Titanium and vanadium complexes were reported later (Scheme 7) [29].

The synthesis of many early transition metals with the C–N–C ligand was greatly facilitated by the isolation and structural characterisation of **36** [4]. The preparation of the ligand in good yields and on a large scale was carried out by deprotonation with KHMDS of the bisimidazolium salts, which were in turn obtained by quaternisation of a variety of substituted imidazoles with 2,6-dibromopyridine (Scheme 7) [4]. The C–N–C ligand has a wide scope of application with the early transition metals supporting complexes of remarkable stability in a range of oxidation states which provide useful platforms for further derivatisation.

Ligands **35** and **37**, obtained similarly, were used to prepare the chromium complexes **40–42** by the reaction with $CrCl_3(thf)_3$. The structure of **40** determined crystallographically (Fig. 6) shows a six coordinate octahedral complex, with Cr–C_{NHC} bond lengths of 2.087(6) and 2.120(6) Å.

The structures of **38** and **39** [30] also feature six coordinate octahedral complexes, with M–C_{NHC} distances of 2.211(5) and 2.191(5) Å (M = Ti) and 2.144(3) and 2.147(3) Å (M = V), respectively. Complex **38** constitutes the only example of a structurally characterised Ti(III)–NHC complex. The V–C_{NHC} bond distances found in **39** fall in the range reported for other V–NHC complexes (2.119(6)–2.132(6) Å) [31].

The niobium complex **43** (Fig. 7) is analogous to complexes **38–42** in containing a six coordinate distorted octahedral geometry around the metal. Complex **43** is the first structurally characterised Nb–NHC complex (Fig. 8) [30].

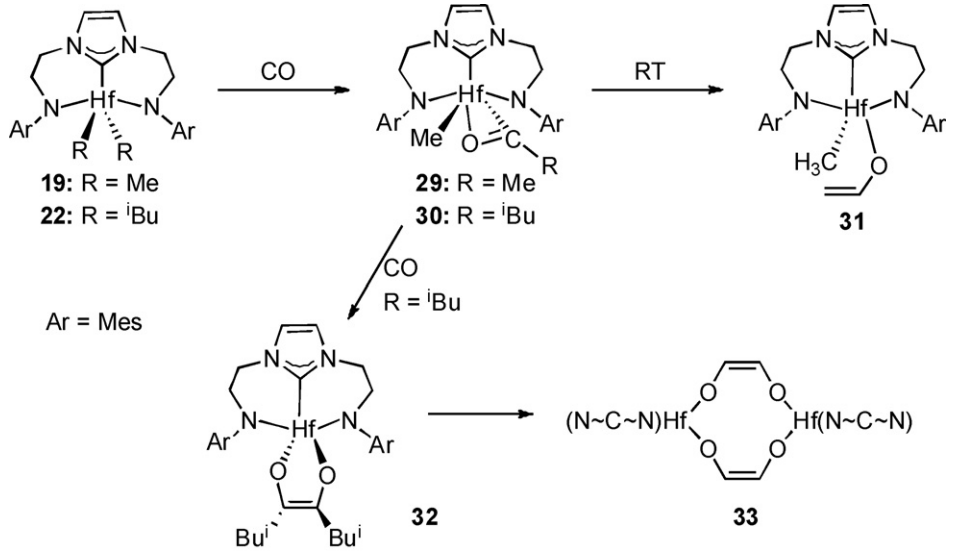

Scheme 6. CO insertion into Hf–C bonds.

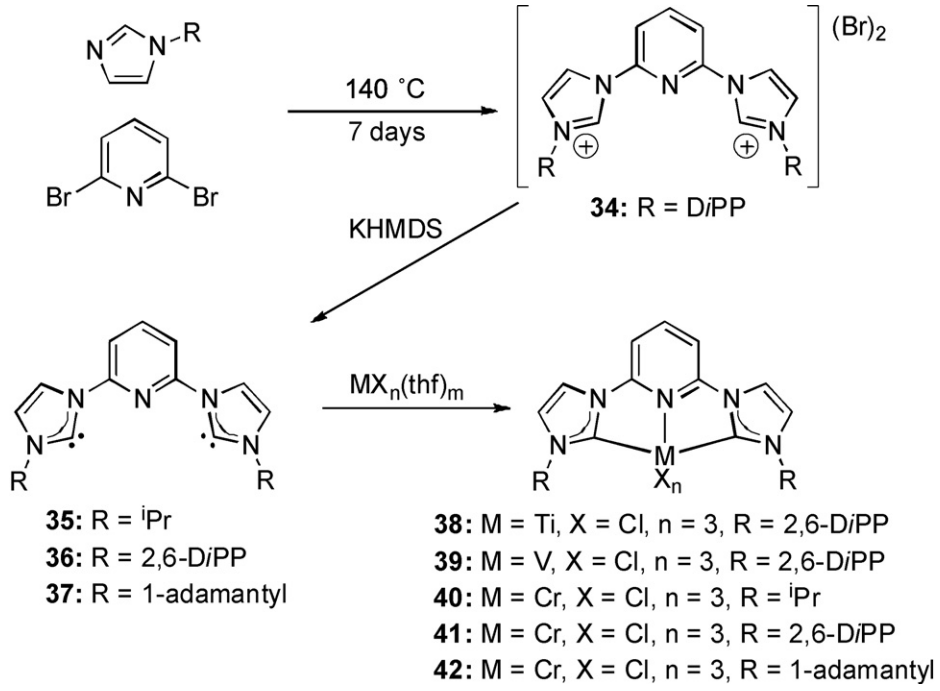

Scheme 7. Synthesis of the C–N–C pincer ligand and complexation to early transition metals.

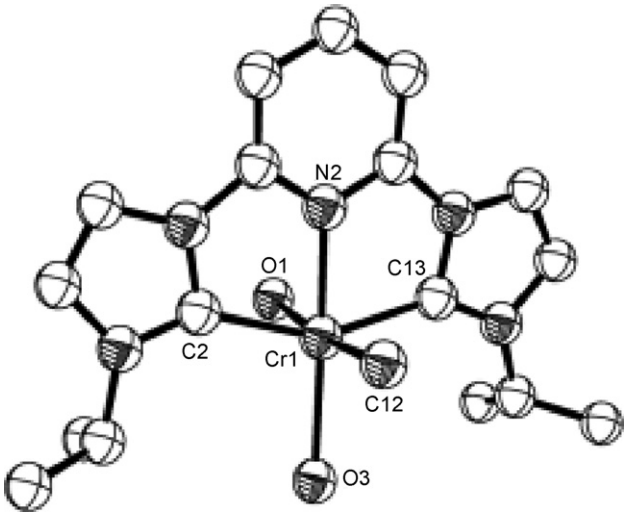

Fig. 6. X-ray structure of **40** [28].

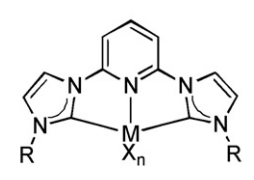

43: M = Nb, X = Cl, n = 3
49: M = Cr, X = Br, n = 2
50: M = Mn, X = Br, n = 2
51: M = U, X = Cl, n = 4

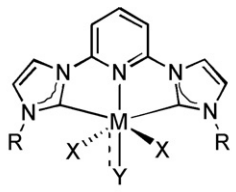

44: M = V, X = Cl, Y = thf
45: M = V, X = Br, Y = thf
46: M = V, X = Cl, Y = O
47: M = V, X = MeCN, Y = O
48: M = Ti, X = Cl, Y = (N^{t}Bu)

Fig. 7. Early transition metal complexes with the C–N–C ligand.

Complexes **44** and **45** are the only two structurally characterised V(II)–NHC complexes. The former was synthesised from the reaction of **36** with $VCl_2(tmeda)_2$ and the latter by halogen exchange of **44** with MesMgBr. Both are six coordinate and adopt a distorted octahedral geometry with *trans* chloride ions and one coordinating thf *trans* to the pyridine nitrogen. The V–C_{NHC} bond lengths of 2.209(9) and 2.162(9) Å in **44** are slightly different, and slightly shorter than for complex **39**. The V–C_{NHC} lengths of 2.227(6) and 2.224(6) Å in **45** are longer than in both complexes **39** and **44**.

Oxidation of **39** and **44** with NMO led to the formation of the vanadium(IV) oxychloride complex **46**. Best yields were obtained using **39** as starting material. Abstraction of the chlo-

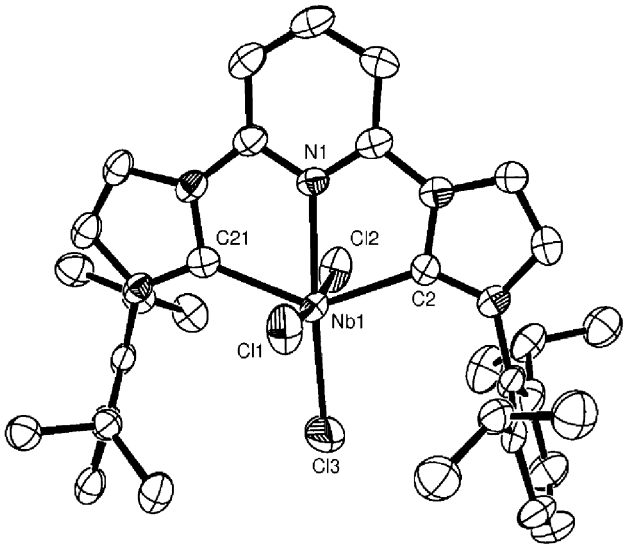

Fig. 8. X-ray structure of **43** [30].

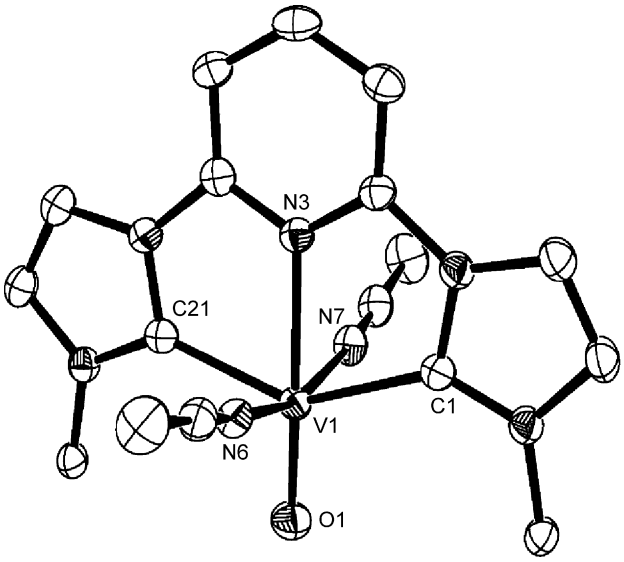

Fig. 9. X-ray structure of **47**; 2,6-D*i*PP groups bar *ipso* carbons and BF_4^- groups omitted for clarity [30].

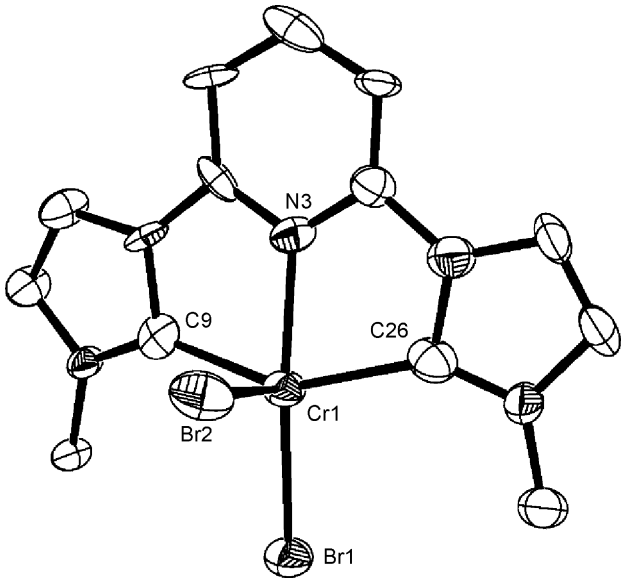

Fig. 10. X-ray diagram of **49**; 2,6-D*i*PP groups bar *ipso* carbons omitted for clarity [30].

ride ions in **46** with $AgBF_4$ in MeCN gave the dicationic V(IV) complex **47** (Fig. 9). Both **46** and **47** adopt a distorted octahedral geometry with the oxide ligand *trans* to the pyridine nitrogen. In **51** the metal cation is coordinated by two MeCN molecules (Fig. 6). V–C_{NHC} bond distances of 2.169(10) and 2.182(11) Å (**46**) are slightly longer than those found in **47**, being 2.129(3) and 2.136(3) Å.

Ti(IV) imido dichloride complex **48** was synthesised by displacement of pyridine from $Ti(N^tBu)Cl_2(py)_3$ by **36**. The $^{13}C\{^1H\}$ NMR signal for the C_{NHC} was seen at 200.72 ppm. The Ti–C_{NHC} bond lengths in **48** are 2.281(6) and 2.286(6) Å, within the range of known Ti(IV)–C_{NHC} bond lengths. However, they are significantly longer than the Ti(III)–C_{NHC} bond lengths in **38** (2.211(5) and 2.191(5) Å). The six coordinate complexes exist in a distorted octahedral geometry similar to **46** and **47**, with the imido moiety *trans* to the pyridine nitrogen.

Treatment of **34** with $Cr(HMDS)_2$ afforded the chromium dibromide complex **49**. This was structurally characterised (Fig. 10), adopting a distorted square-based pyramidal geometry (τ value of 0.29 indicating substantial distortion). The Cr–C_{NHC} bond lengths of 2.125(10) and 2.122(10) Å are within the known range of Cr(II)–NHC bonds (2.091(2)–2.127(5) Å) [32]. The analogous (C–N–C)$CrCl_2$ complex was synthesised by reacting $CrCl_2$ with **36**, but no structural characterisation was obtained.

The manganese dibromide complex **50** was synthesised from the reaction of **36** with $MnBr_2$. It adopts a five coordinate, distorted square-based pyramidal geometry (the τ value of 0.12 indicating that the distortion is not as severe as other five coordinate pincer complexes). The Mn–C_{NHC} bond lengths of 2.206(2) and 2.210(2) Å are similar to the other known Mn(II)–C_{NHC} bonds (2.210(4)–2.270(2) Å) [33,34].

The only pincer carbene complex of an f-block metal is the uranium complex **51**. It was synthesised from the reaction of UCl_4 and **36** and was structurally characterised (Fig. 11). It adopts a seven coordinate geometry best described as a distorted capped trigonal prism, with Cl1, Cl3 and C21 forming one triangular face; Cl2, Cl4 and C21 forming the other triangular face and N1 being the capping ligand. Cl2 and C21 are connected by an edge, as are C2 and Cl1 and Cl2 and Cl4. The U–C_{NHC} bond lengths of 2.573(5) and 2.587(5) Å are shorter than in other U(IV)–C_{NHC} complexes (2.636(9)–2.799(3) Å) [35,36].

The only report of C–C–C pincer complexes appeared in 2005, when Hollis reported the synthesis and characterisation

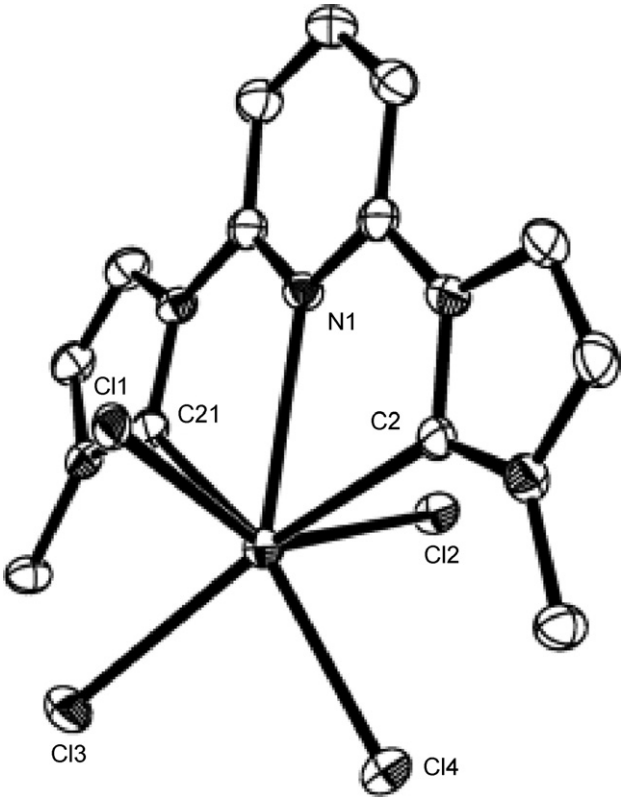

Fig. 11. X-ray structure of **51**; 2,6-D*i*PP groups bar *ipso* carbons omitted for clarity [30].

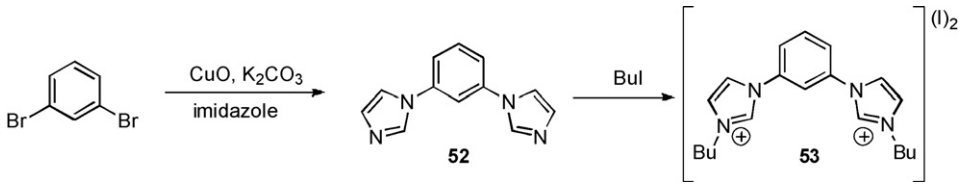

Scheme 8. Synthesis of the C–C–C pincer proligand.

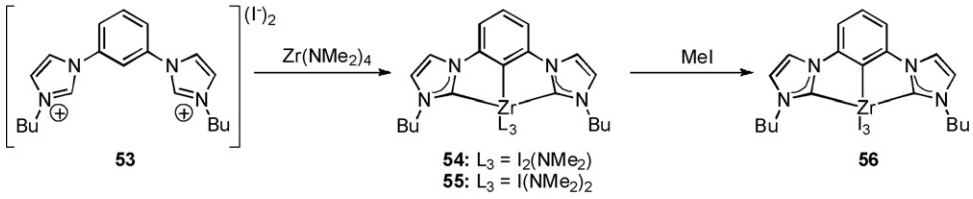

Scheme 9. Synthesis of the (C–C–C)$ZrCl_3$ complex **56**.

of Zr and Rh complexes of both saturated and unsaturated pincer ligands [37]. The bis-imidazolium salt precursor **53** was synthesised by reacting 1,3-dibromobenzene with imidazole in the presence of base and CuO catalyst. Quaternisation of the bis-imidazole **52** with ^{n}butyl iodide led to **53** in good yield (Scheme 8).

Metallation of **53** was accomplished by stirring with 2.5 equiv. of $Zr(NMe_2)_4$ for 10 min in DCM. This formed the (C–C–C)$Zr(NMe_2)_2$I complex **54** in good yield, with a small amount of byproduct (9% in the solid state) being the mono-amido bis-iodide **55** (Scheme 9). Reaction of this mixture of products with MeI yielded the triiodide complex **56**.

Both **54/55** and **56** (Fig. 12) were characterised by single crystal X-ray diffraction and NMR spectroscopies. The ^{13}C NMR signals of the carbene carbons were seen at 188.9 ppm (**54/55**) and 195.5 ppm (**56**). The Zr–C_{NHC} bond lengths of 2.4256(10) and 2.3990(11) Å (**54/55**) and 2.334(3) and 2.335(3) Å (**56**) are all within the expected range.

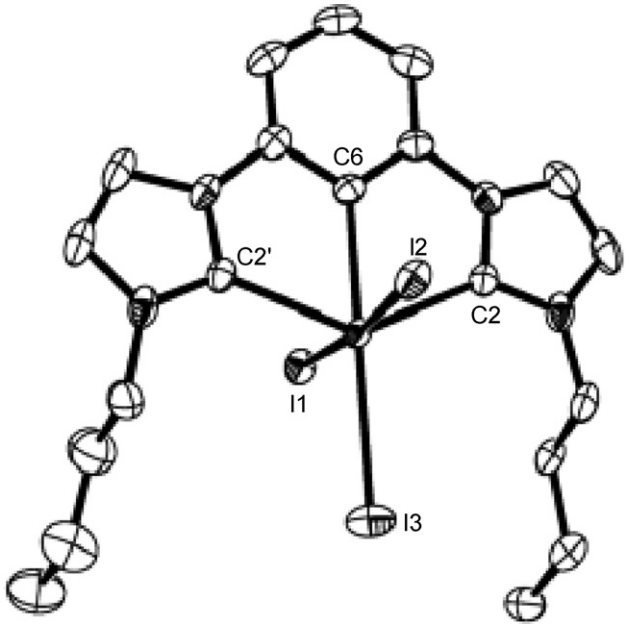

Fig. 12. X-ray structure of **56** [85].

The saturated analogue of salt **53** was synthesised by condensation of *N*-acetyl-glycine with *m*-phenylenediamine, followed by reduction with $LiAlH_4$, cyclisation with $HC(OEt)_3$ and anion exchange with $NaBPh_4$ (Scheme 10). Salt **57** was metallated with 5 equiv. of $Zr(NMe_2)_4$ in benzene, which was activated by stirring with mesityl lithium for 10 min prior to addition of the salt, forming Zr complex **58** [37].

Although Zr complex **58** was not structurally characterised, the ^{13}C NMR signal for the C_{NHC} was found at 211.8 ppm.

2.3. Catalytic reactions of early transition metal complexes with NHC pincer ligands

The polymerisation of olefins catalysed by non-metallocene systems has been an active area of research in recent years [38]. The catalytic activity of some early transition metal complexes of NHC pincer ligands towards olefin polymerisation has been studied, and the catalyst rated according to the classification system devised by Gibson and co-workers [39].

Preliminary studies on the catalytic activity of complex **4** were carried out. In the presence of 1000 equiv. of MMAO, under 9 bar of ethylene at 30 °C for 30 min, **4** was found to be a highly active procatalyst. The activity was found to be 290,000 g mol^{-1} h^{-1} bar^{-1}, or 'very high' [18].

Reaction of ^{mes}(N$^-$∼C∼N$^-$)$ZrMe_2$ (**17**) with $[Ph_3C][B(C_6F_5)_4]$ resulted in the formation of the monocationic derivative, which was then tested for ethylene polymerisation activity. An activity of 123 g mol^{-1} h^{-1} bar^{-1} was reported, which is considered 'high'. However, on exposure to ethylene, an exotherm was noticed, suggesting that the active species was short-lived. The same cationic zirconium species, along with the analogous hafnium derivative from **18**, were also tested for 1-hexene polymerisation activity. After workup, atactic poly-1-hexene was recovered in just 4% yield [24].

The chromium complexes **40–42** were tested for ethylene polymerisation activity with varying pressures and amounts of MAO. Complex **41** gave the highest activi-

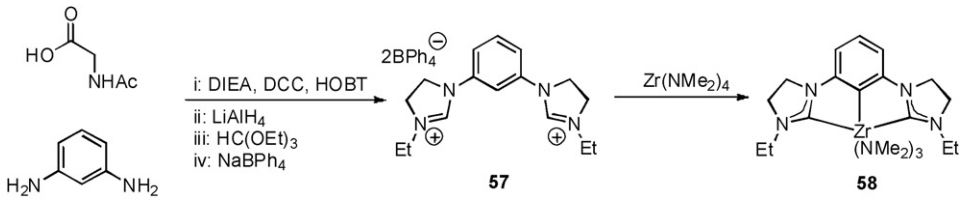

Scheme 10. Synthesis of the saturated C–C–C pincer proligand and the (C–C–C)Zr(NMe$_2$)$_3$ complex **58**.

ties of polymerisation, consistently 'very high' but a maximum of 40,400 g mmol^{-1} h^{-1} bar^{-1} with a 1000:1 ratio of MAO:Cr complex and 3000 equiv. of Al(^{i}Bu)$_3$ as scavenger. Complex **42** showed a low activity and **40** managed 1394 g mmol^{-1} h^{-1} bar^{-1} (very high) with 1 bar ethylene and 500 equiv. MAO [28].

The activities of **38** and **39** were lower than the (C–N–C) $CrCl_3$ complex **41**, but were still classed as mainly 'high'. At 1 bar, **39** managed 1280 g mmol^{-1} h^{-1} bar^{-1} (500 equiv. MAO) and 1446 g mmol^{-1} h^{-1} bar^{-1} (500 equiv. co-MAO), both classed as 'very high' levels of activity [29].

However, by far the most active catalyst was **4**, which was over seven times more active than **41**.

3. Group 11 metal complexes

Even though silver–NHC complexes have not found any use as NHC transfer reagents to early transition metals [40] they played a major role in the development of NHC-late transition metal chemistry and therefore are discussed before the late transition metals. The preferred coordination geometries of Ag(I) and Cu(I) centres lead to bidentate or monodentate binding modes of the ligands of Fig. 2 and formation of mono-, bi- or tri-nuclear complexes, hence the notation of 'pincer' ligand is meaningless in this section. There are no gold complexes with the ligands of Fig. 2.

3.1. Silver complexes

Silver–NHC complexes are easily prepared by the reaction of imidazolium salts with silver containing bases (most frequently Ag_2O, but also AgOAc and Ag_2CO_3). They are usually air stable and cleanly transfer the NHC ligand to late transition metals under mild conditions, the reaction being driven by the precipitation of silver halide salts. Furthermore, the Ag–NHC complexes exhibit interesting structural and catalytic chemistry and have useful medicinal activity. The intense research activity that followed Lin's report on the synthesis of simple Ag–NHC complexes by the action of Ag_2O on imidazolium salts [3] has been recently presented in a detailed review, which also includes a systematic classification of the structurally characterised complexes in five structural motifs [41]. The metal environment in the majority of the reported complexes comprise either one cationic Ag centre coordinated by two NHC ligands, commonly observed when non-coordinating anions are employed, or one neutral Ag centre coordinated by one NHC ligand and one coordinating anion, usually halide. The coordination geometry at the metal is linear, sometimes slightly distorted. When the non-coordinating anion is $[Ag(halide)_2]^-$, bimetallic interactions involving the metal centres of the cation and the anion have been observed. In a few cases, the formation of oligonuclear silver clusters is supported by the NHC-containing ligand structure. In this review we shall limit our discussion to silver complexes with the ligands shown in Fig. 2.

Silver complexes with the ligands C^N^C (R = Me (**59**) [42], Bu^n (**60**) [43], mesityl (**61**), 2,6-D*i*PP (**62**) [10]), C–N–C (R = Me (**63**) [9], benzyl (**64**) [44], mesityl (**65**), 2,6-D*i*PP (**66**) [10]), C∼N∼C (R = Bu^t, **67**) [45], ox^C–ox (**68**) [46], P∼C∼P (**69a–c**) [47], C^O$^-$^C (R = Bu^t, **70**) [48] and py^C^py (**71a–b**) [49] have been synthesised, characterised by analytical and spectroscopic methods and used further in transmetallation reactions. The lability of the NHC–Ag complexes and the dependence of their constitution and structure on the solvent and the anion limits our knowledge of the nature of the species in non-polar, non-coordinating solvents, unless crystallographic information is directly available. The invaluable information from the electrospray mass spectrometry is usually obtained by sample preparation in acetonitrile, in which redistribution of the NHC ligands is favoured [50], usually leading to the observation of molecular ions containing the $[Ag(NHC)_2]^+$ groups not necessarily present in non-coordinating solvents. Even though the C_{NHC} in the $^{13}C\{^1H\}$ NMR spectra of the silver complexes has been observed in many cases, its position cannot be used as a highly diagnostic tool of the coordination environment of the silver. In most complexes the C_{NHC} appears in the range 175–185 ppm, with the cationic species towards the lower field end of the range. Fluxionality [3], concentration [50] and relaxation effects make the observation of the C_{NHC} sometimes problematical.

The most commonly used method for the preparation of the silver carbene complexes involves the reaction of the corresponding imidazolium salts (halides, BF_4^-, BPh_4^-, NO_3^-) with Ag_2O (usually in excess) in chlorinated solvents and rarely in acetonitrile, dichloromethane/acetonitrile mixtures or methanol [51]. The reaction can be accelerated at refluxing temperatures or in the presence of dehydrating agents (activated 4 Å molecular sieves, $MgSO_4$, etc.). Starting from imidazolium halides, the initially formed products in chlorinated solvents usually contain the NHC–Ag–halide functionality, are occasionally contaminated by inorganic impurities (**59**) [42] and can have limited solubility in organic solvents if the NHC substituents are not lipophilic (**60**) [43]. Further reaction with AgY (Y = BF_4^-, NO_3^-) can abstract the halides coordinated to the metal (**59**) [42], exchange a halide counterion (**69**) [52] or introduce more Ag centres that may coordinate with other donors of the ligand (**71**) [49]. In rare cases,

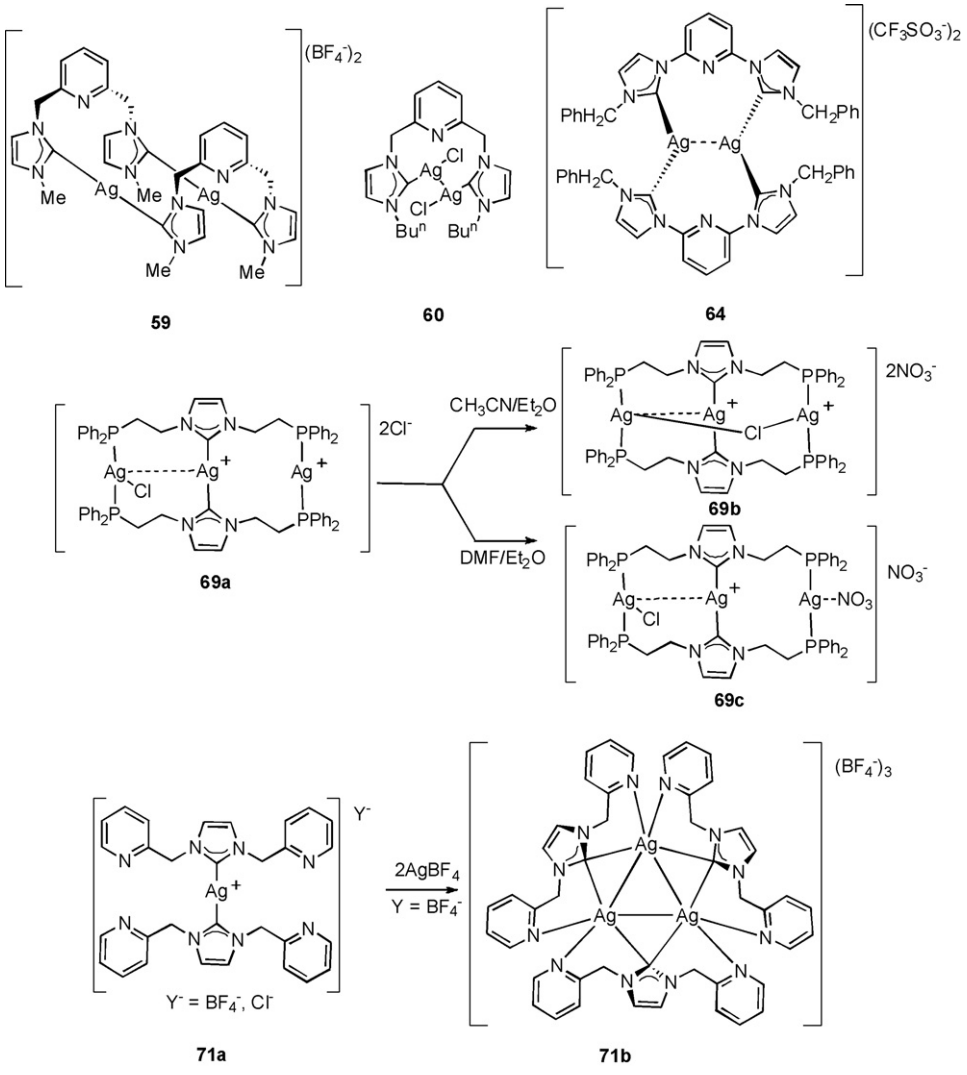

Fig. 13. Crystallographically characterised silver complexes with the rigid tridentate ligands.

the silver complexes have been prepared by *in situ* generation of the free carbene from the imidazolium salt with KOBu^t in thf followed by trapping with AgOTf (**64**) [44].

Detailed crystallographic data are only available for the complexes which are shown in Fig. 13.

The structurally characterised complexes with the C^N^C ligands are either monomeric (**60**) or dimeric (**59**). The former (R = Bu^n) feature two Ag centres coordinated with one NHC and one chloride ion in an almost linear geometry [43]. The proximity of the metal centres gives rise to Ag–Ag interactions (2.374(3) Å), substantially shorter than the sum of the van der Waals radii of Ag (3.44 Å, argentophilicity) (Fig. 14). There is no interaction between the $N_{pyridine}$ and silver.

A variation of the C^N^C ligand system (R = Me), in combination with non-coordinating anions in the solid state gave rise to dimeric ionic species of the type $[Ag_2(C^N^C)_2](BF_4)_2$, (**59**) containing Ag centres bridging the two C^N^C ligands *via* linear $Ag(NHC)_2$ functionalities [42]. Here too there is no interaction between the $N_{pyridine}$ and silver. In this structure

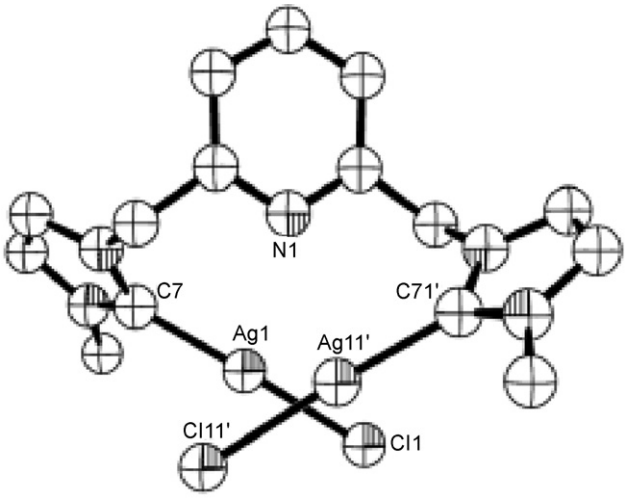

Fig. 14. The structure of the monomeric complex **60** [43].

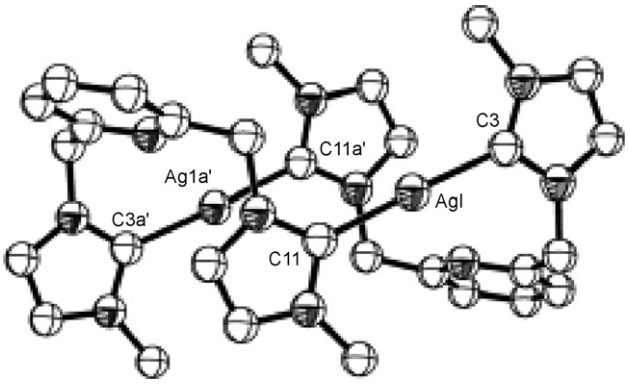

Fig. 15. The structure of the cation in **59** [42].

the Ag–Ag interaction is much weaker (3.7171(5) Å) [42]. The Ag–C_{NHC} distances are within the expected range for metal carbon single bonds (2.065–2.085 Å) (Fig. 15).

There is only one crystallographically characterised salt with the C–N–C ligand system (R = CH_2Ph, **64**) [44]. The anions are non-coordinating triflates while the cation adopts a dimeric structure $[(C–N–C)_2Ag_2]^{2+}$, comprising linear $Ag(NHC)_2$ units analogous to the ones reported above (Fig. 16).

The silver complex with the C∼N∼C ligand has been synthesised by the reaction of the imidazolium salt with excess of Ag_2O. It exhibits a polymeric structure in the solid state with bridging C∼N∼C ligand and linear NHC–Ag–NHC functionalities; there is no amine–silver interaction [98].

The precursor to complex **69a**, a P∼CH∼P imidazolium salt, was synthesised from the reaction of 1,2-dichloroethane with imidazole and base, quaternisation with 1,2-dichloroethane and phosphorylation with $PHPh_2$ and base (Scheme 11) [47].

The structures of the silver complexes with the P∼C∼P ligand are dependent on the nature of the anion and the solvents of crystallisation [52]. The ionic species containing a non-symmetric trinuclear cation is obtained from the reaction of the imidazolium salt with Ag_2O in dichloromethane and was formulated as $[(P∼C∼P)_2Ag_3Cl](Cl)_2$ (**69a**) based on spectroscopic evidence. Anion exchange of the chloride with NO_3^- gave two different ionic complexes **69b** and **69c**, the cations of which contain three Ag centres in a linear arrangement with different coordination spheres around each silver atom and different ligand backbone conformations. The complexes (Figs. 17 and 18) can be isolated by crystallisation from different solvent systems.

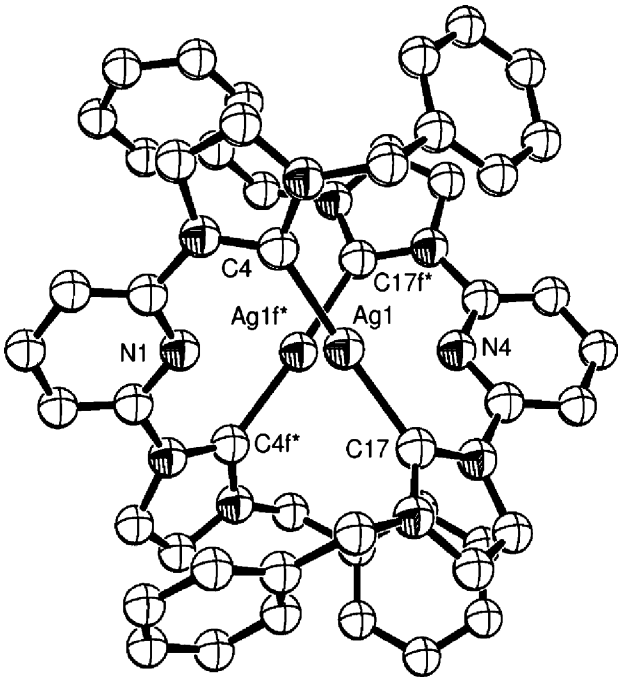

Fig. 16. The structure of the cation in **64** [44].

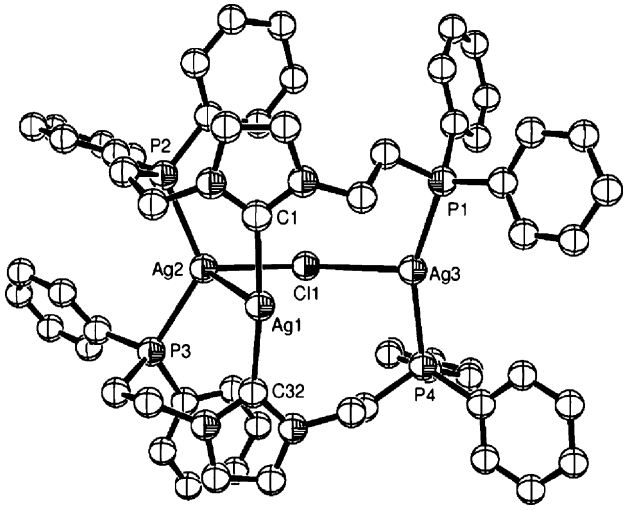

Fig. 17. The structure of the cation **69b** in the trinuclear complexes; Ar groups (bar *ipso* carbons) omitted for clarity [52].

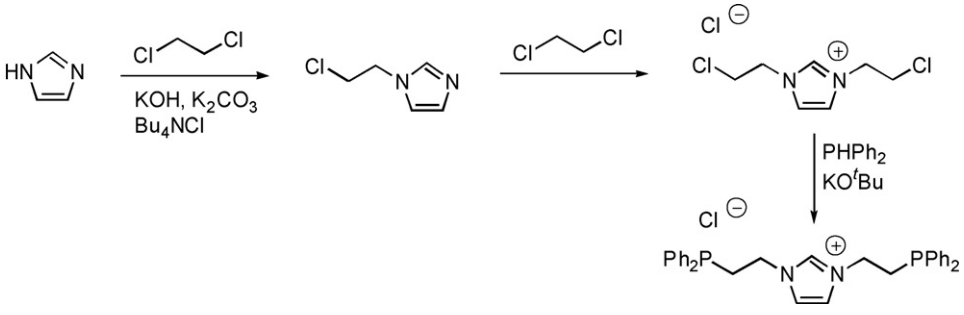

Scheme 11. Synthesis of the P∼CH∼P proligand.

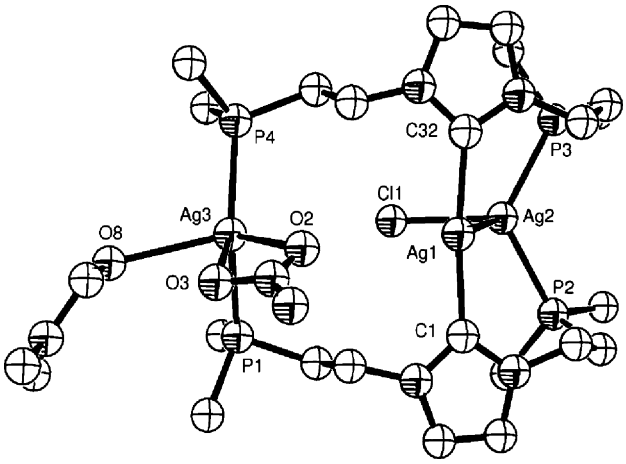

Fig. 18. The structure of the cation **69c** in the trinuclear complexes; Ar groups (bar *ipso* carbons) omitted for clarity [52].

The structures of the silver complexes supported by the py^C^py ligand show interesting features [49]. The complex (**71a**) initially obtained from the reaction of the imidazolium salt (as Cl^- or BF_4^-) with Ag_2O features the well established quasi-linear $Ag(NHC)_2$ arrangement with dangling pyridine functionalities. In the chloride salt, the intermetallic distances observed (Ag–Ag = 3.650 Å) preclude argentophilic interactions; isolated cations are seen in the BF_4^- salt (Fig. 19).

Addition of excess $AgBF_4$ to **71a** in acetonitrile or direct reaction of the imidazolium tetrafluoroborate with excess of $AgBF_4$ gave a new ionic species (**71b**) with a trinuclear cation in which the silver centres occupy the corners of an equilateral triangle with strong argentophilic interactions (Ag–Ag = 2.72–2.77 Å). In addition, the pairs of silver atoms are bridged by NHC ligands and two pyridine groups (Fig. 20).

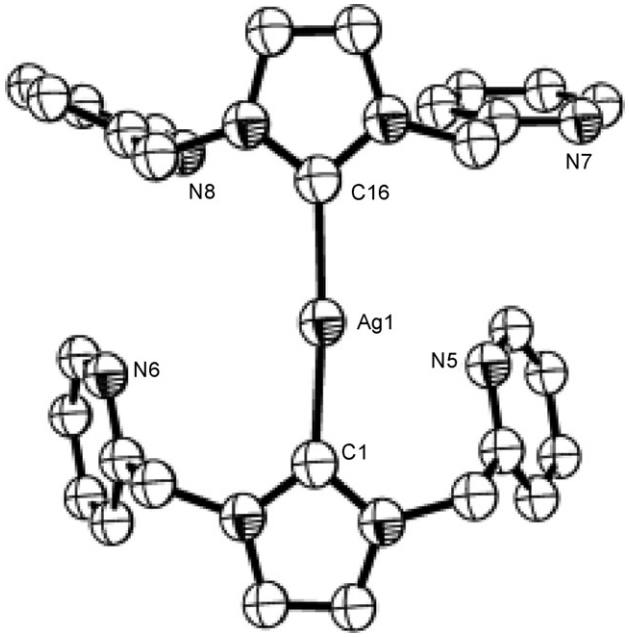

Fig. 19. The structure of the cation in **71a** [49].

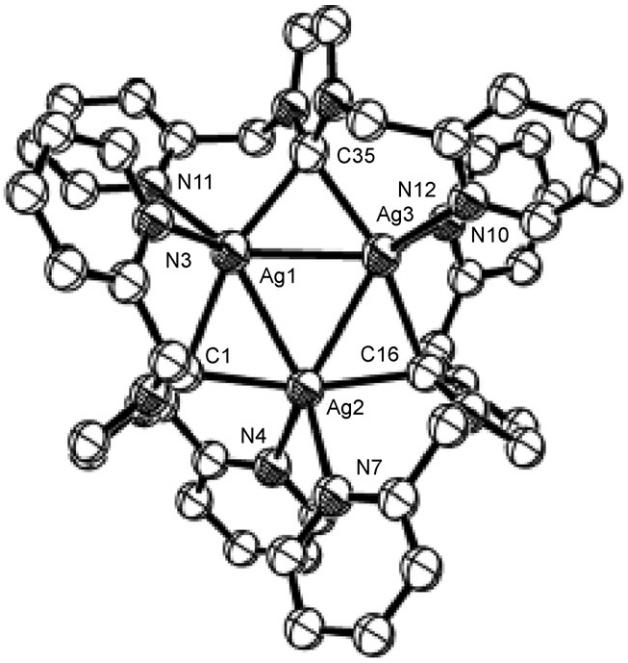

Fig. 20. The structure of the cation in **71b** [49].

The planes of the imidazole heterocycles are almost perpendicular to the Ag_3 plane, giving the complex an overall D_{3d} symmetry with alternate coordination of the pyridine moieties above and below the plane of the Ag_3 triangle. Bridging NHCs are extremely rare. In addition to the symmetrically bridging NHCs discussed here, two more complexes have been reported with bridging NHC groups. In the Ag paracyclophanes a non-symmetric bridging coordination mode of the NHC is observed [53], while the FcP^C^FcP compound **73** supports an NHC ligand symmetrically bridging two copper(I) centres (*vide infra*) [54].

A similar structure has been recently reported for the py^C^py analogue (R = CH_2OH) [51]. The Ag–Ag, Ag–C_{NHC} and Ag–$N_{pyridine}$ distances are similar to complex **71b**.

Although a polymeric (C∼N∼C) Ag complex was synthesised by Arnold and co-workers [55] the ligand has not been utilised to form a 'pincer' complex with other metals and is therefore excluded from this review.

3.2. Copper complexes

In comparison to the ubiquitous silver complexes, the number of copper complexes with rigid linear tridentate and 'pincer' *N*-heterocyclic carbene ligands is limited. They are summarised below (Fig. 21).

Complex **72** was prepared by the reaction of the free (C–N–C) with CuBr in dichloromethane, followed by anion exchange with $NaBPh_4$ and crystallisation from dichloromethane/ether [56]. The ^1H NMR spectrum of the complex at room temperature exhibits broad lines due to fluxionality. The structure in the solid state is shown in Fig. 22.

The complex is ionic, with the cation comprising two copper centres in three- and five-coordination environments. The three coordinate centre (two NHC and one Cu–Cu interaction)

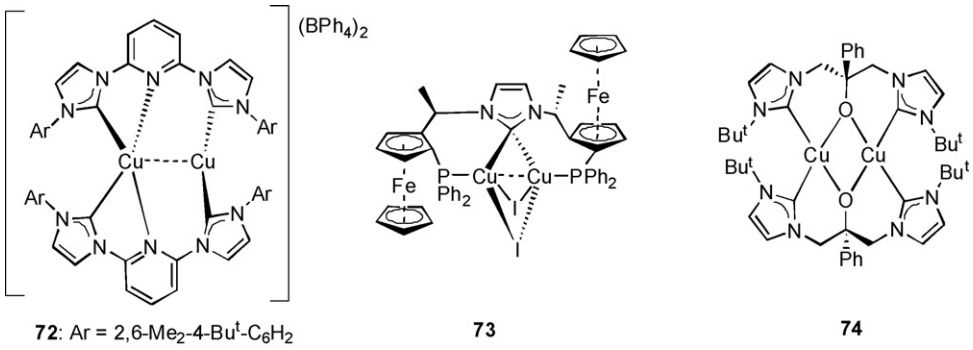

Fig. 21. Crystallographically characterised copper(I) complexes with the rigid tridentate ligands.

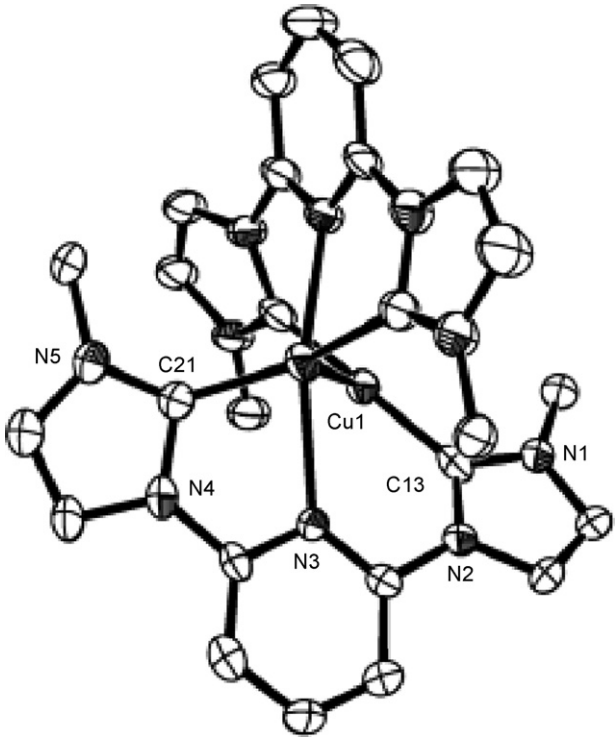

Fig. 22. The structure of **72** [56].

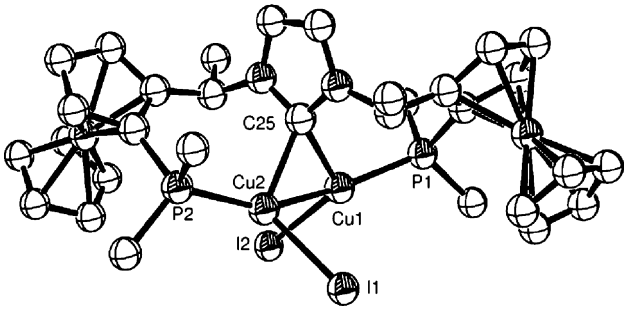

Fig. 23. The crystal structure of **73**; Ph groups bar *ipso* carbons omitted for clarity [54].

adopts a T-shaped geometry with the C_{NHC}–Cu–C_{NHC} vector being almost linear. The five coordinate centre adopts a distorted square pyramidal geometry. The Cu–C_{NHC} bond lengths are within the range reported for other copper carbene complexes [57]. However, the Cu–$N_{pyridine}$ distances are rather long (ca. 2.32 Å). The Cu–Cu separation (2.694 Å) suggests a weak bimetallic interaction.

The C_2 symmetric chiral (FcP^C^FcP) with flexible linkers was introduced by Togni as an example of chiral ligands with NHC functional groups. The imidazolium proligand was prepared in a multistep sequence by deprotonation of *N*,*N*-dimethyl-1-ferrocenylethylamine with ^{n}BuLi, followed by quenching of the lithiated ferrocene derivative with chlorodiphenylphosphine and acetylation with acetic anhydride leading to **75**. This was then reacted with imidazole in the presence of water, followed by ion exchange with NaI, affording the imidazolium salt **76** (Scheme 12).

The copper complex with the FcP^C^FcP ligand (**73**) was prepared by the reaction of the imidazolium salt **76** with copper(I) acetate in THF followed by the addition of Bu_4NI, or by the reaction of the free carbene generated *in situ* (from **76** and $NaOBu^t$ in THF) with $CuI(PPh_3)$. Spectroscopic evidence (NMR spectroscopy and electrospray mass spectrometry) supports a dinuclear complex formulation with one FcP^C^FcP ligand in a C_2 symmetric geometry [54]. The structure in the solid state (Fig. 23) is in agreement with the spectroscopic assignment and constitutes a unique example of an *N*-heterocyclic carbene ligand symmetrically bridging two copper centres, even though bridging NHC ligands have been observed in silver complexes on two occasions (*vide supra*).

Finally, the tridentate ligand C^O$^-$^C has been introduced to Cu(I) metal centres by the reaction of the corresponding silver carbene complex with copper iodide [48]. The structure of **74** in

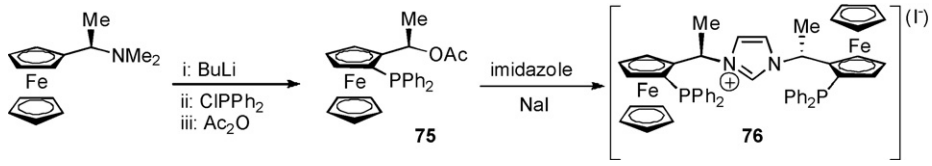

Scheme 12. Synthesis of the imidazolium salt (FcP^CH^FcP)$^+$.

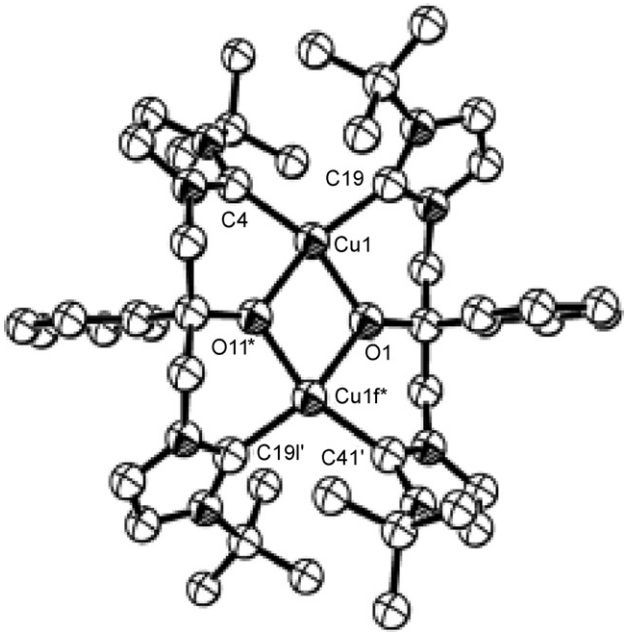

Fig. 24. The structure of **74** [48].

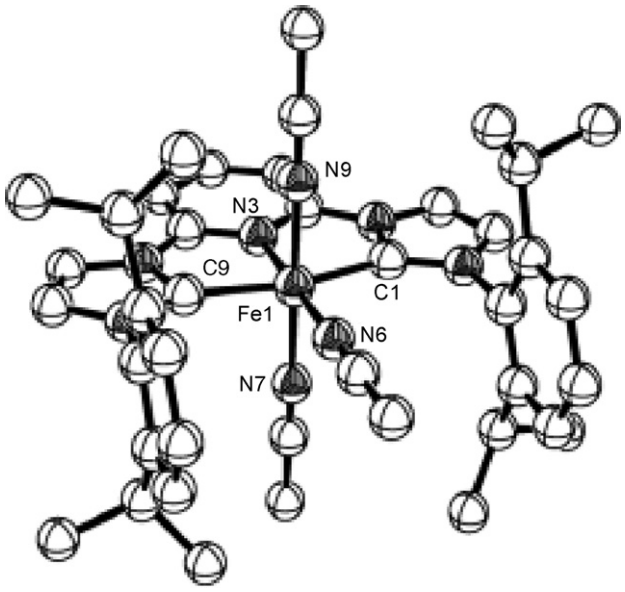

Fig. 25. X-ray structure of **78** [58].

the solid state (Fig. 24) shows the presence of a binuclear system with coordination of the NHC groups and two bridging alkoxides. The Cu(I) centres exhibit distorted square planar geometry with Cu–C_{NHC} at the long end of the range for Cu(I)–NHC bonds.

4. Group 8 metal complexes

To date, there have been no reports of pincer ligands with an NHC functionality complexed to osmium. Therefore, in this section we describe the iron and ruthenium complexes.

4.1. Iron complexes

Pincer NHC complexes of iron are rare, with only one type of ligand, the (C–N–C), having given an interesting class of complexes in various oxidation states. Attempts to prepare the (C–N–C)$FeCl_2$ complex by the direct reaction of ligand **36** with $FeCl_2(PPh_3)_2$ or $FeCl_2(thf)_{1.5}$ did not yield the expected product [58]. Instead, the complexes [(C–N–C)FeCl(thf)]$_2$[$FeCl_4$] and [(C–N–C)FeCl(PPh_3)]$_2$[$FeCl_4$] were formed; these were further reacted with $NaBPh_4$ in MeCN to form the dicationic species **78** and **79** (Scheme 13).

An X-ray diffraction study of **78** showed a distorted octahedral species, with one (C–N–C) ligand and three acetonitrile ligands filling the coordination sphere (Fig. 25). The Fe–C_{NHC} bond lengths of 1.944(5) and 1.947(5) Å are within the range of known Fe(II)–C_{NHC} bonds (1.933(8)–2.194(10) Å) [58]. The reaction was also carried out using a slightly different pincer ligand (R = 2,6-dimethyl-4-*tert*-butylphenyl, **77**); this gave **79** as an analogous product.

Reaction of ligand **36** with [$FeCl_2$(tmeda)]$_2$ again failed to yield the desired (C–N–C)$FeCl_2$ complex. However, the ionic products **80** or **81** isolated this time comprised a cation with two

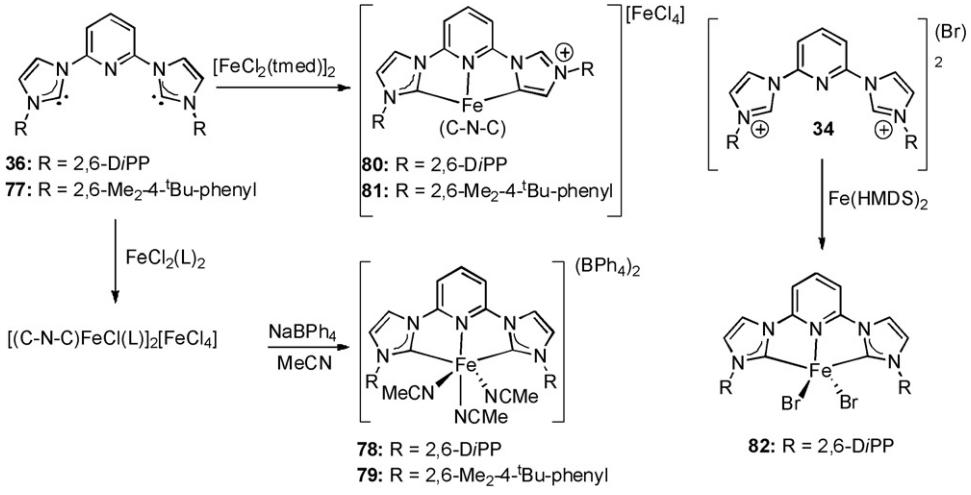

Scheme 13. Synthesis of (C–N–C)$FeBr_2$ complex **82**.

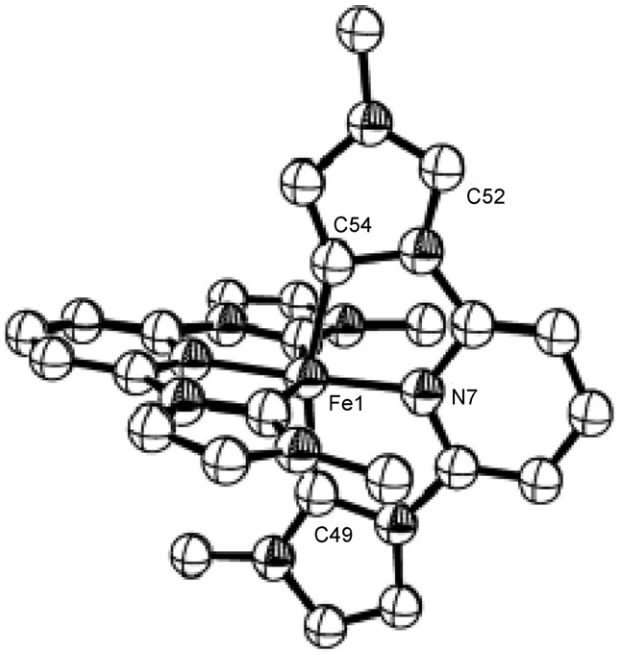

Fig. 26. X-ray structure of **81**; aryl groups except *ipso* carbons omitted for clarity [58].

tridentate ligands; in one of them the NHC group had undergone C–H activation at the C4 imidazol-2-ylidene backbone carbon. Structural characterisation of the 2,6-dimethyl-4-*tert*-butylphenyl analogue **81** was carried out (Fig. 26). This shows a distorted octahedral geometry around the Fe centre, with two pincer ligands. One coordinates in a conventional manner and the other coordinates through a carbene via the C2 carbon, pyridine N and a carbene via the C4 carbon. This unusual ('abnormal') binding mode has been firstly observed with pyridine functionalised iridium carbene complexes [59] and has also been observed with other metal/ligand combinations (Cu, Pd, etc.). In the present case the driving force to 'abnormal' coordination may be of steric origin. The Fe–C_{NHC} distances of 1.933(8), 1.938(8) and 1.938(8) Å are at the lower range of known Fe(II)–C_{NHC} bond lengths. No NMR data was obtained due to the paramagnetic nature of the anion.

The desired (C–N–C)$FeBr_2$ complex was finally obtained as a purple paramagnetic solid from the reaction between $Fe(HMDS)_2$ and the imidazolium dibromide salt **34** (Scheme 13). The structure of **82** (Fig. 27) reveals a five coordinate iron centre in a distorted square-based pyramidal geometry (τ value of 0.33 indicates substantial distortion). The Fe–C_{NHC} bond lengths of 2.193(10) and 2.166(10) are the longest Fe(II)–C_{NHC} bond lengths known.

Complex **82** was also prepared from the direct reaction of **36** with $FeBr_2$ at low temperatures [29] and its identification was based on analytical data. Similarly, the (C–N–C)$FeCl_3$ complex **83** was obtained from the dicarbene **36** and $FeCl_3$. However, when the less sterically congested pincer **35** was reacted with $FeBr_2$, the $[(C–N–C)_2Fe][FeBr_4]$ complex **84** was formed (Fig. 28). Unlike **80** and **81**, no 'abnormal' metallation of the carbene ring was seen in **84** possibly due to the less sterically congested metal centre. The Fe–C_{NHC} bond lengths of 1.952(2) and 1.959(2) Å are within the known range of Fe(II)–C_{NHC} bond lengths.

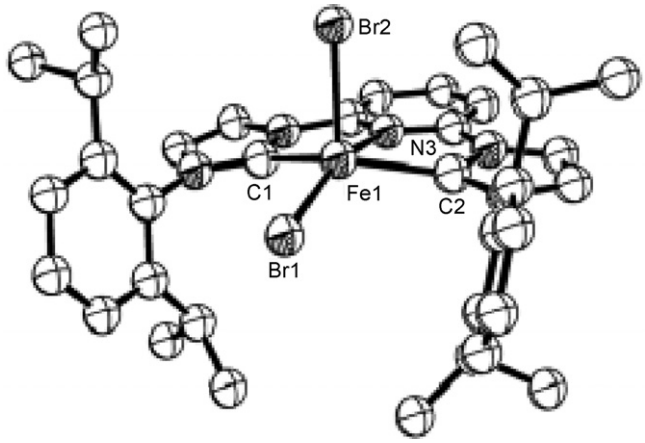

Fig. 27. X-ray structure of **82** [58].

Reduction of **82** with Na/Hg under 5 bar pressure of N_2 yielded the Fe(0) dinitrogen complex **85**. This was the first metal dinitrogen complex stabilised by an NHC ligand and was structurally characterised (Fig. 29).

Complex **85** is a five coordinate distorted square-based pyramidal species (τ value of 0.02 indicates minimal distortion). Both N_2 ligands bind in an end-on fashion, with N–N bond distances of 1.113(3) and 1.115(3) Å slightly longer than in free N_2 (1.0968 Å). The Fe(0)–NHC bond lengths of 1.912(3) and 1.915(3) Å are considerably shorter than the only other structurally characterised Fe(0)–NHC complex (2.007 Å) [60]. The coordinated dinitrogen molecule shows moderate 'spectroscopic activation' as indicated by the position of the $\nu(N_2)$ at 2109 and 2031 cm^{-1}.

Complex **85** was reacted with CO, ethylene and PMe_3, with all the products being structurally characterised (Scheme 14).

All three complexes **86–88** are five coordinate distorted square-based pyramidal, with τ values ranging from 0.18 (**86**)

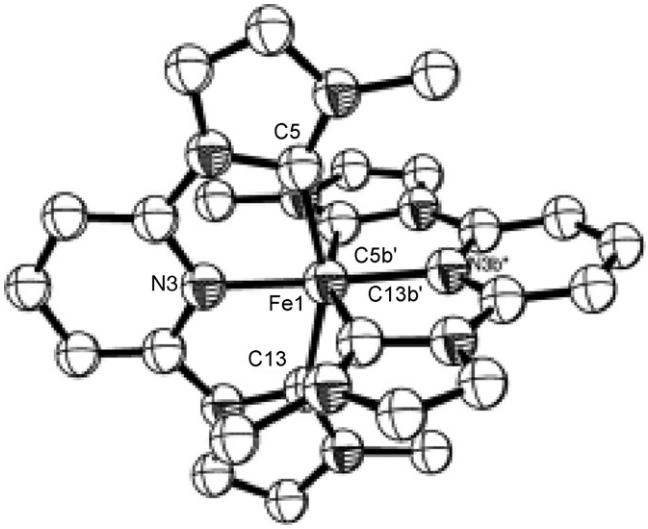

Fig. 28. X-ray structure of the cation in complex **84**; aryl groups except *ipso* carbons omitted for clarity [29].

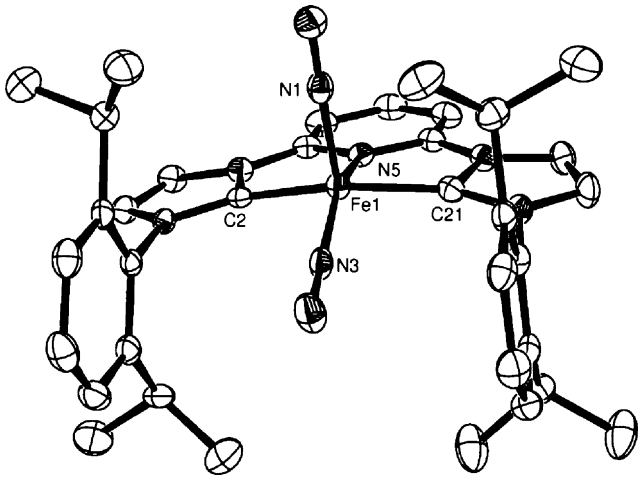

Fig. 29. X-ray of the N_2 complex **85** [98].

to 0.28 (**87**). In complex **86** both N_2 molecules were replaced by CO, but reaction of **85** with both ethylene and PMe_3 resulted in substitution of only one N_2 molecule. In both cases, the incoming ligand is found in the axial position.

The Fe(0)–C_{NHC} bond lengths of 1.910(3) and 1.918(3) Å (**86**), 1.927(6) and 1.933(6) Å (**87**) and 1.881(3) and 1.888(3) Å (**88**) are all shorter than the only previously known Fe(0)–C_{NHC} bond length [60]. The reported ^{13}C NMR signals for the C_{NHC} are 203.87 (**9**), 210.43 (**86**), 210.78 (**87**) and 208.56 (**88**).

4.2. Ruthenium complexes

Perhaps the most famous example of a metal complex containing an NHC ligand is the Grubbs second-generation metathesis catalyst [61]. However, there are very few examples of pincer NHC complexes of ruthenium. Their catalytic activity has only partially been explored.

The first example of a ruthenium complex with an NHC pincer ligand was reported in 2002 [4]. Reaction of ligand **36** with $RuCl_2(PPh_3)_3$, afforded the (C–N–C)$RuCl_2(PPh_3)$ complex **89** which was structurally characterised (Fig. 30). The Ru centre in **89** adopts a distorted octahedral geometry with the two chloride ions being mutually *cis*. There is an obvious distortion of the 2,6-D*i*PP groups, bending away from perpendicular to the plane of the ligand backbone (dihedral angle of 11.67°) in order to accommodate the steric bulk of the PPh_3 ligand. The Ru–C_{NHC} bond lengths of 2.025(8) and 2.028(8) Å are within the range of known Ru(II)–C_{NHC} bond lengths for unsaturated NHCs of 1.967(5)–2.168(2) Å [62,63].

The (CH–N–CH)Br_2 bis-imidazolium bromide **91** (R = ^{n}Bu) serves as a source of carbene for the preparation of (C–N–C)$RuBr_2$(CO) from $[RuCl_2(COD)]_n$ in the presence of triethylamine in ethanol (Scheme 15) [64]. The resultant product (**92**) was structurally characterised and showed a distorted octahedral complex, with two mutually *cis* bromide ions and one CO ligand. The CO was thought to originate from the oxidative addition of acetaldehyde followed by methyl group migration and

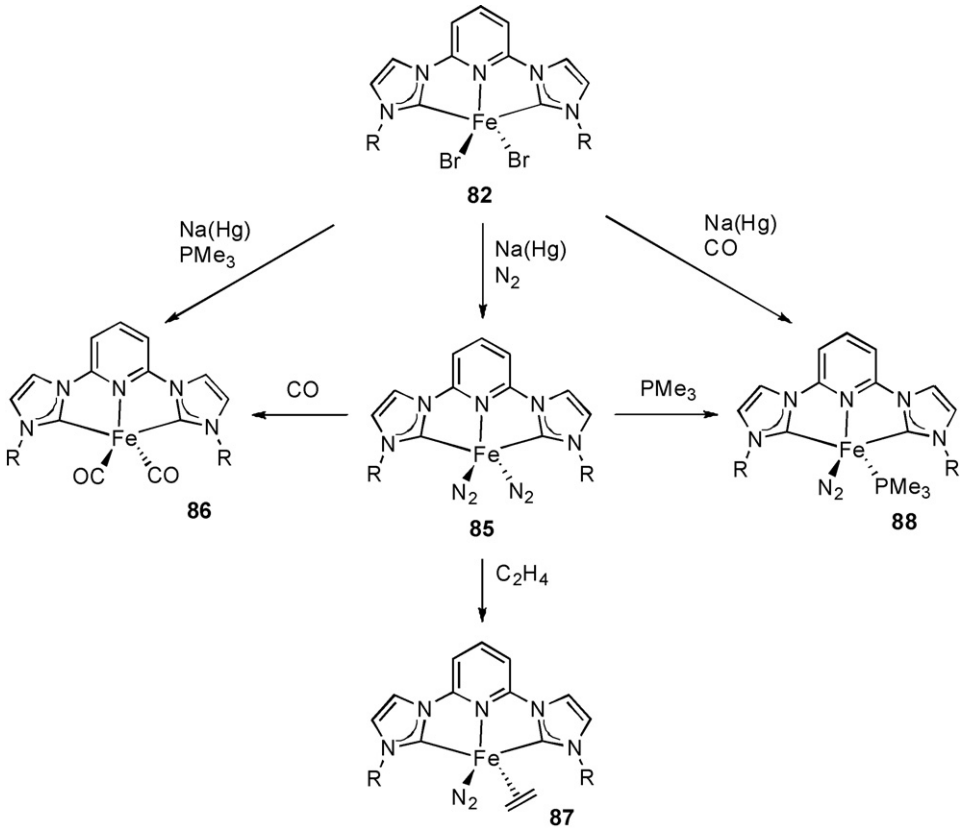

Scheme 14. Reactivity of the (C–N–C)$Fe(N_2)_2$ complex **85**.

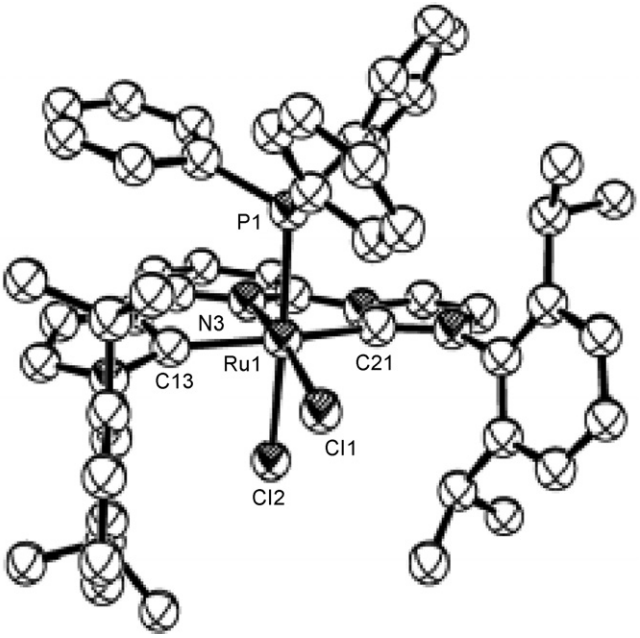

Fig. 30. X-ray structure of (C–N–C)$RuCl_2(PPh_3)$ complex **89** [4].

methane elimination. The Ru–C_{NHC} bond lengths of 2.062(5) and 2.056(5) Å are within the range of known Ru(II)–C_{NHC} bond lengths. The CO stretching frequency of 1922 cm^{-1} suggests minimal back donation to the carbene carbon.

When salt **91** was heated with commercial $RuCl_3$ and purified by elution through silica with DCM/acetone/KPF_6, the $[(C–N–C)_2Ru][PF_6]_2$ complex **93** was formed. This was also structurally characterised (Fig. 31), showing the presence of a distorted octahedral dicationic complex with non-coordinating PF_6 anions.

The Ru–C_{NHC} bond lengths of 2.052(7), 2.057(7), 2.061(7) and 2.068(7) Å are within the range of known Ru(II)–C_{NHC} bond lengths. The ^{13}C NMR signals for the C_{NHC} are observed at 197.2 ppm (**92**) and 188.7 ppm (**93**).

A similar (R = Me) [11] $[Ru(C–N–C)_2](PF_6)_2$ salt was reported by Chung and co-workers [65]. Complex **95** was prepared by the addition of the imidazolium salt to hydrated $RuCl_3$ in the presence of a halide abstractor at 190 °C (Scheme 16). Various abstractors were used, but the only structurally characterised compound contained BPh_4^- anions from $NaBPh_4$. The Ru–C_{NHC} bond lengths of 2.048(2), 2.0486(19), 2.053(2) and 2.0551(19) Å are all within the range of known Ru(II)–NHC bond lengths.

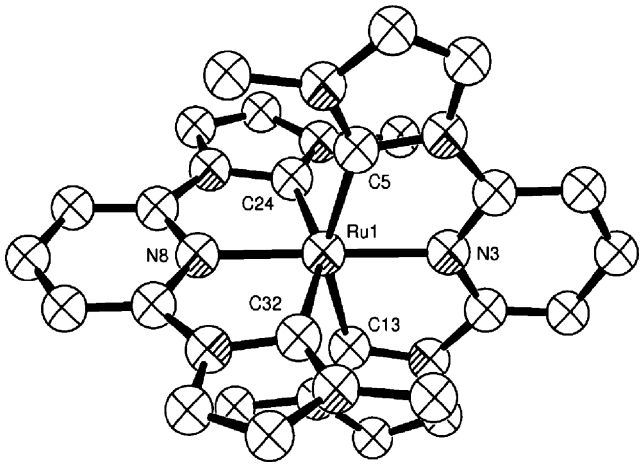

Fig. 31. X-ray structure of 2:1 Ru complex **93** [64].

Deprotonation of the imidazolium salt **76** with NaO^tBu, followed by reaction of the carbene generated *in situ* with $RuCl_2(PPh_3)_3$ yielded the (FcP^N^FcP)Ru(Cl)(I) complex **96**. The presence of the facially coordinating ligand was deduced from the ^{31}P NMR spectra showing two phosphorus environments ($J_{P–P}$ = 28 Hz) indicating a *cis* relationship. The crystal structure of **96** confirmed the *facial* coordination mode in a five coordinate square-based pyramidal geometry. However, upon reaction with 1 equiv. of $[OEt_3]PF_6$ in the presence of MeCN, the chloride ion was selectively abstracted and an octahedral complex resulted. Although no structural characterisation became available, analysis of the ^{31}P NMR spectrum revealed only one ^{31}P environment, in accordance with the presence of a C_2-symmetric species. The ^{13}C NMR signal for the C_{NHC} was found at 167.2 ppm, slightly lower than for **96** at 178.7 ppm.

The interconversion between facial and meridional coordination involving the linear tridentate ligands was also seen in the ruthenium complexes with the (P∼C∼P) ligand introduced by Chiu and Lee [52]. Reaction of the silver complex **69** with $RuCl_2(PPh_3)_3$ resulted in the formation of a dimeric species with three bridging chloride ions between two octahedral ruthenium centres, the *fac*-ligands completing the ruthenium coordination spheres. This $[(P∼C∼P)_2Ru_2(\mu\text{-}Cl)_3]Cl$ product (**97**) was also synthesised by the direct reaction of the imidazolium salt with $RuCl_2(PPh_3)_3$.

Reaction of the dimer **97** with phenylacetylene resulted in the formation of a six coordinate monomeric species. The $^{31}P\{^1H\}$ NMR spectrum showed just one resonance, indicating a C_2-symmetric species with meridional coordination of the

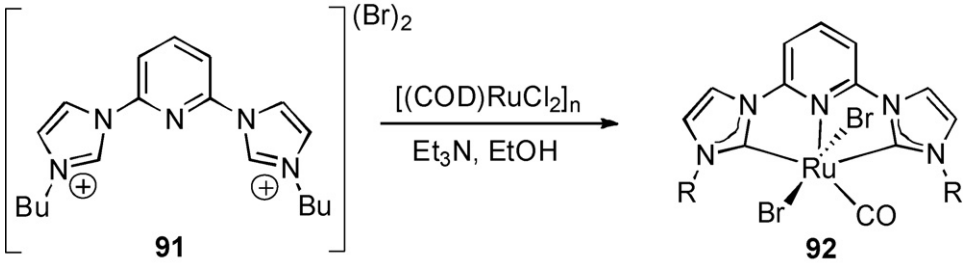

Scheme 15. Synthesis of the (C–N–C)$RuBr_2$(CO) complex **92**.

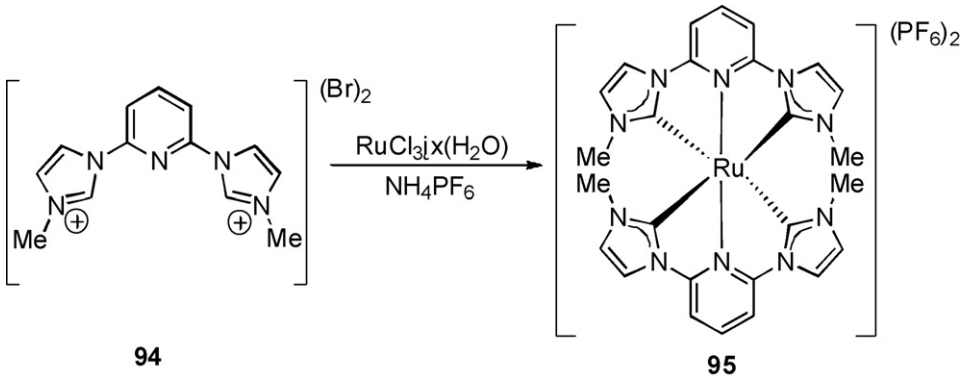

Scheme 16. Synthesis of $[(C–N–C)_2Ru](PF_6)_2$.

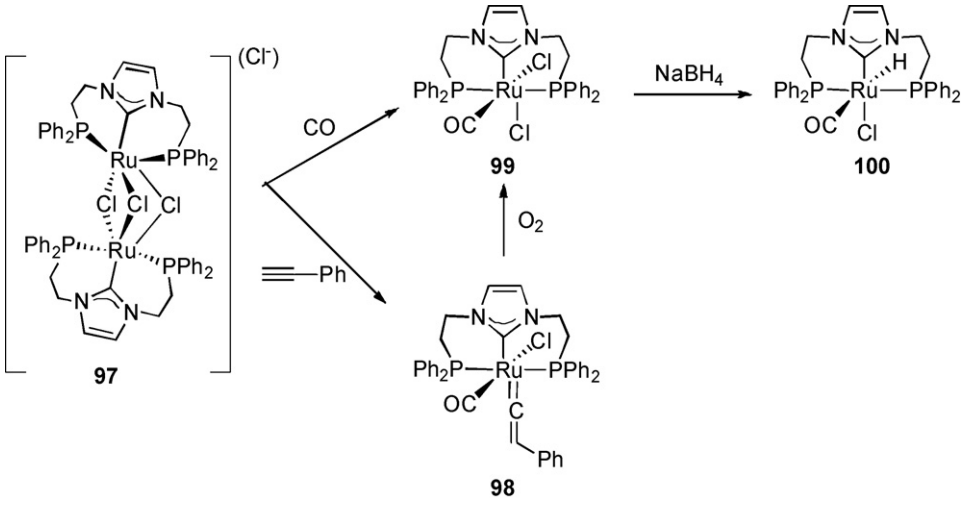

Scheme 17. Reactivity of the facially coordinating dimer **97**.

(P∼C∼P) ligand. The presence of a vinylidene species (**98**) was assigned on the basis of a ^{13}C NMR signal at 348.1 ppm for the vinylidene carbon (Scheme 17). The vinylidene group is *trans* to the carbene with mutually *trans* chloride ions completing the coordination sphere.

The reaction of **97** with CO also resulted in a meridionally coordinated ligand: complex **99** is octahedral with mutually *cis* chloride ions and one CO. Refluxing the vinylidene complex **98** in air resulted in cleavage of the vinylidene group, also forming carbonyl **99**. Reduction of **99** with $NaBH_4$ in EtOH formed the ruthenium hydride species **100**. The proposed structure of **100** was based on ^{31}P and ^{1}H NMR data which support a meridional coordination mode for the (P∼C∼P) ligand and the hydride *trans* to the chloride ion.

The dimer **97** was also reacted with both pyridine and bipy. The bipy product retained the facially coordinating ligand geometry of the dimer, but the product of the pyridine reaction was complex **101**, which was structurally characterised (Fig. 32).

Complex **101** is a six coordinate octahedral complex with two pyridine ligands, one coordinated chloride ion and one uncoordinated chloride ion. The pyridine ligands are *trans* to each other with the coordinated chloride ion *trans* to the NHC. The $Ru–C_{NHC}$ distance of 2.027(7) Å is within the range of known $Ru–C_{NHC}$ bonds. Reaction of **101** with bipy resulted in a change from *mer* to *fac* coordination of the tridentate ligand and displacement of both py ligands with bipy. If exposed to air, **101** is oxidised to the (P∼C∼P)$RuCl_3$ complex **102**, which was also structurally characterised. The *mer* geometry is retained and the $Ru–C_{NHC}$ distance of 2.050(4) Å is within the range of known $Ru–C_{NHC}$ bonds.

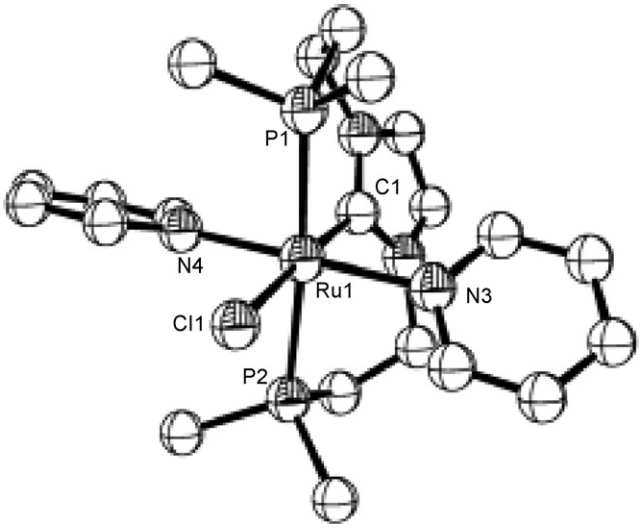

Fig. 32. X-ray of (P∼C∼P)RuCl(py)Cl, complex **101**; Ph groups except *ipso* carbons omitted for clarity [52].

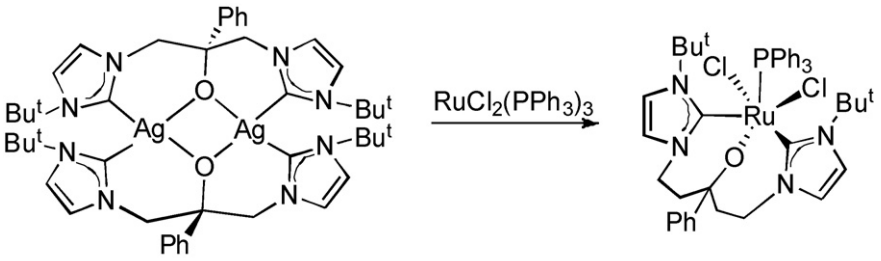

103

Scheme 18. Synthesis of facially coordinating (C^O^{-}^C)$RuCl_2(PPh_3)$, **103**.

Finally, the tridentate (C∼O∼C) ligand reported by Arnold was only seen to coordinate in a facial geometry, giving rise to an unusual organometallic Ru(III) centre (Scheme 18) [66].

4.3. Catalytic reactions

The Fe complexes **82** and **83** were tested for catalytic activity in ethylene polymerisation reactions but all proved inactive [29]. Complex **82** did, however, prove to be an active catalyst for the coupling of aryl Grignards with primary and secondary alkyl halides [67]. The coupling of *p*-tolyl magnesium bromide and cyclohexyl bromide produced the desired 4-cyclohexyltoluene in 94% yield, with only a small amount of the di-*p*-toluene as byproduct. Coupling of the same Grignard with 4-methylcyclohexyl bromide resulted in 89% conversion to the desired product and with *n*-octyl bromide, a 71% conversion was observed [4].

The majority of the ruthenium complexes were tested for catalytic activity in transfer hydrogenation reactions. Complex **89** was most active for the reduction of cyclohexanone in isopropanol at 55 °C, with a turnover number of 8800 (0.01 mol% catalyst, 20 h, KO^{t}Bu as base), although it also showed good activity for acetophenone (TON = 4000) at 80 °C (0.015 mol%, 12 h, KO^{t}Bu) and benzylidene aniline (TON = 4200) at 55 °C (0.015 mol%, 20 h, KO^{t}Bu).

However, the complex **92** reported by Peris was more active for the reduction of cyclohexanone. At 80 °C, **92** exhibited a TON of 126,000 (0.0007 mol%, 20 h, KOH). It was less reactive towards acetophenone though, with a TON of just 700 (0.07 mol%, 6 h, KOH) [64]. None of the pincer complexes **97**–**99** were tested for catalytic activity, but the facially coordinated ruthenium dimer **97** did show reasonable activity for the transfer hydrogenation of cyclohexanone and acetophenone.

Complex **95** was also tested for catalytic activity in the oxidative cleavage of olefins. With 1 mol% catalyst and 1.25 equiv. of $NaIO_4$ at RT, electron rich olefins (methylcyclohexene, norbornene, geraniol) were cleaved into the corresponding aldehydes/ketones in >99% yield. The same catalyst was less reactive towards electron poorer olefins (stilbene, styrene) [65].

5. Group 9 metal complexes

As already mentioned in the previous section, there are no published examples of complexes with pincer ligands bearing NHC groups with 5d metals. Therefore, in this section we describe work on cobalt and rhodium complexes.

5.1. Cobalt complexes

The only reported pincer complexes of Co containing an NHC moiety contain the (C–N–C) ligand system [68]. They are conveniently prepared by aminolysis of $Co(HMDS)_2$ by the imidazolium salt (CH–N–CH)Br_2 **34**, resulting in the formation of (C–N–C)$CoBr_2$ (**104**) a five coordinate paramagnetic Co(II) complex (Scheme 19). No structural characterisation was possible; however, the reactivity of **104** towards substitution, oxidation and reduction was described.

Reaction of **104** with TlOTf in pyridine gave the paramagnetic octahedral Co(II) complex **105**. The triflate groups are mutually *cis* to the NHC functionalities with one pyridine *trans* to the pyridine of the pincer completing the coordination sphere. The Co–C_{NHC} bond lengths of 1.942(6) and 1.941(6) Å are within the range of known Co(II)–C_{NHC} bonds (1.902(3)–2.080(5) Å) [69,70].

The attempted alkylation of **104** with 4 equiv. of MeLi did not yield a Co(II) alkyl complex, but rather it was accompanied by reduction, giving the Co(I) methyl complex **106**. This was also synthesised from the reduction of **104** with Na/Hg, forming the Co(I) bromide **107**, followed by alkylation with MeLi. Both **106** and **107** are four coordinate diamagnetic square planar complexes in the solid state (Fig. 33).

The Co–C_{NHC} bond lengths of 1.917(5) and 1.909(5) Å (**106**) and 1.914(4) and 1.898(4) Å (**107**) are within the range of known Co(I)–C_{NHC} bond lengths (1.875(8)–2.0545(14) Å) [70,71]. Although the complexes were diamagnetic, the C_{NHC} signal was not observed in the $^{13}C\{^1H\}$ NMR spectrum.

Oxidation of **104** with $BrN(TMS)_2$ resulted in the formation of a six coordinate octahedral Co(III) complex **108**. The Co–C_{NHC} bond length of 1.962(7) Å is within the range of known Co(III)–C_{NHC} bond lengths (1.914(2)–2.043(2) Å) [72,73]. Due to the low solubility of the compound, no ^{13}C NMR data were obtained.

5.2. Rhodium complexes

The first report of a rhodium pincer NHC complex came in 1995, with Matsumura's series of bis(thiolato)carbene ligands derived from 10-*S*-3 tetraazapentalenes [74]. Double deprotonation of 3,4,5,6-tetrahydro-2-pyrimidine thiol (**109**) with ^{n}BuLi, followed by reaction with 2-chloroacetophenone and a substi-

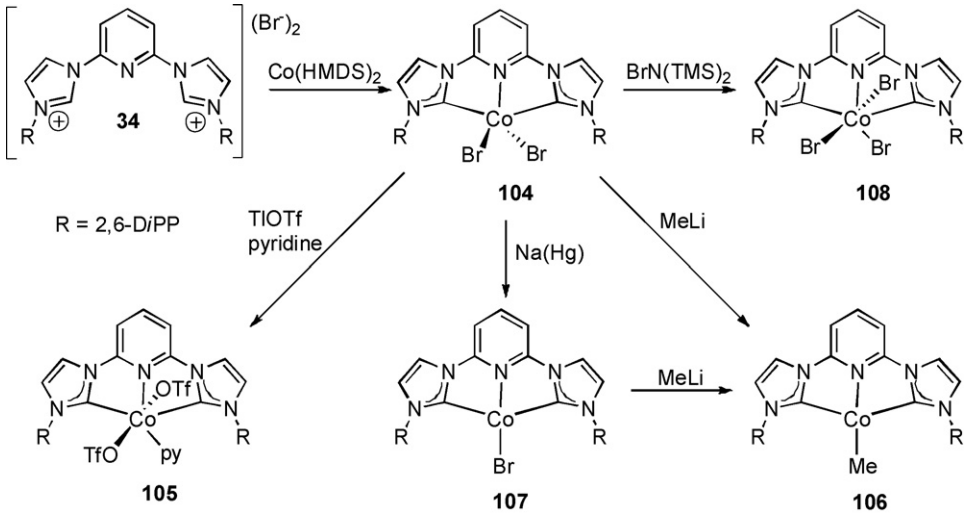

Scheme 19. Synthesis and reactivity of (C–N–C)$CoBr_2$ complex **104**.

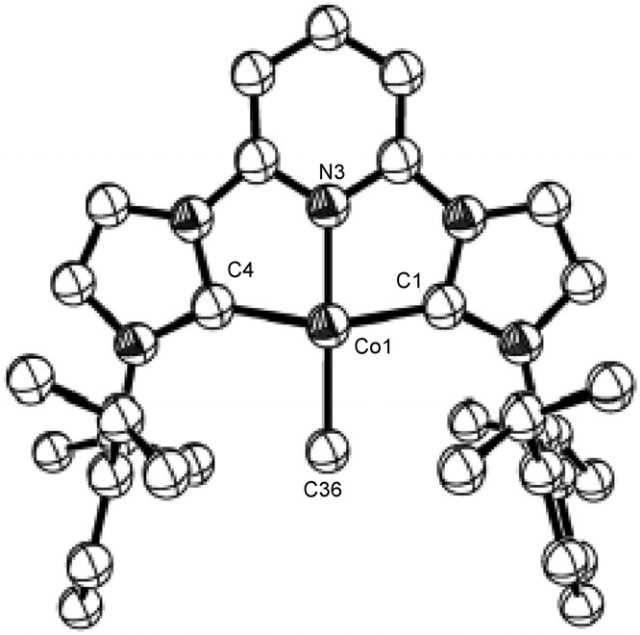

Fig. 33. The structure of (C–N–C)CoMe **106** [68].

tuted isothiocyanate resulted in the formation of the relevant tetraazapentalene **110** (Scheme 20) [75].

Stirring **110** with $RhCl(PPh_3)_3$ in benzene/DCM (1:1) for 72 h resulted in the formation of an octahedral Rh(III) complex (Scheme 21). The type of product was dependent on the nature of R, with aryl complexes yielding the symmetric product **112**, and alkyl complexes the unsymmetric product **111**. The six-membered NHC ring found within this ligand set is the only six-membered NHC ring found as part of a 'pincer' ligand and has not been synthesised by alternative synthetic routes.

Complex **111a** was structurally characterised, showing a six coordinate octahedral Rh(III) centre with meridionally coordinating ligand. The Rh–C_{NHC} bond distance of 1.937(5) Å is within the range of known Rh(III)–C_{NHC} bonds (1.915(15)–2.087(11) Å) [76,77]. Complex **112c** was structurally characterised later [78]. The Rh–C_{NHC} bond lengths of 1.930(10) and 1.933(5) Å were also within the range of known Rh(III)–C_{NHC} bond lengths (Fig. 34).

Structures where one or both of the thiocarbonyl functionalities were replaced by carbonyls were reported in a subsequent article [79]. If one thiocarbonyl functionality was replaced, then an unsymmetric (S^-–C–N^-) pincer analogous to **111** was obtained. However, if both thiocarbonyls were replaced, the carbene was not formed (Scheme 22).

Structural characterisation of **114** confirmed the presence of a six coordinate octahedral Rh(III) species with non-symmetric 'pincer' ligand. The Rh–C_{NHC} bond length of 1.940(7) Å was within the range of known Rh(III)–C_{NHC} bonds.

A diselenato version of ligand **110** with a five-membered ring was formed in an analogous way, with the relevant isoseleno-

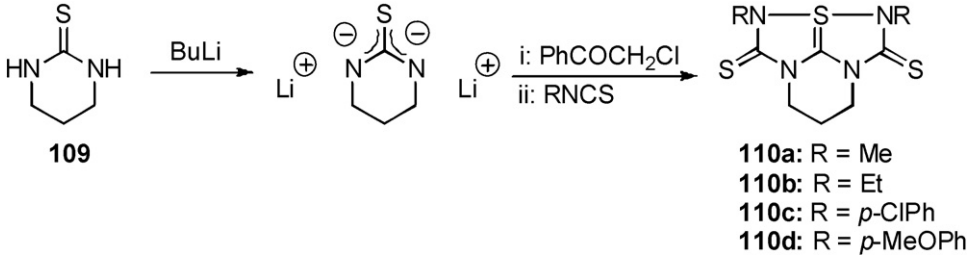

Scheme 20. Synthesis of the tetraazapentalene proligand **110**.

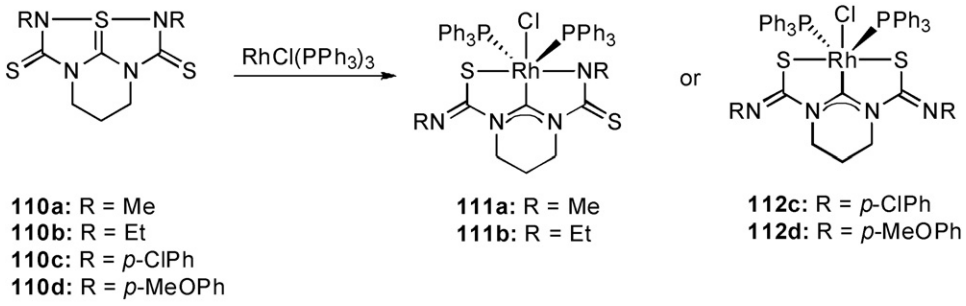

Scheme 21. Formation of (S–C–N)RhCl(PPh$_3$)$_2$ and (S–C–S)RhCl(PPh$_3$)$_2$ complexes.

cyanate being used instead of isothiocyanate [80]. Reaction of ligand **117** with RhCl(PPh$_3$)$_3$ resulted in the formation of **118**, a six coordinate octahedral Rh(III) species with symmetrical (Se$^-$–C–Se$^-$) pincer (Scheme 23). The Rh–C$_{NHC}$ bond length of 1.941(9) Å is within the range of known Rh(III)–C$_{NHC}$ bond lengths.

Gade reported the synthesis of the imidazolium proligand (Ox–C^Ox)(Br) by the reaction sequence shown in Scheme 24. The imidazolium salt has been converted to the silver complex **68** by the reaction with Ag$_2$O.

The rhodium complex with the ligand (ox)–C^(ox), was prepared from **119** and [Rh(O^{t}Bu)(nbd)]$_2$ in thf [46]. Oxidation with bromine at −78 °C resulted in the synthesis of the Rh(III) complex **120** (Scheme 25).

Complex **120** was structurally characterised, showing the presence of a six coordinate distorted octahedral geometry at the

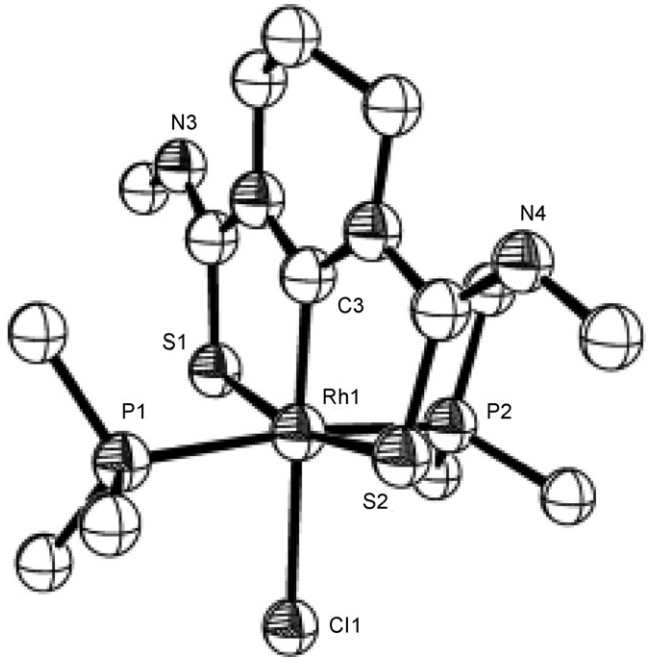

Fig. 34. X-ray structure of **112c**; Ar groups bar *ipso* carbons omitted for clarity [99].

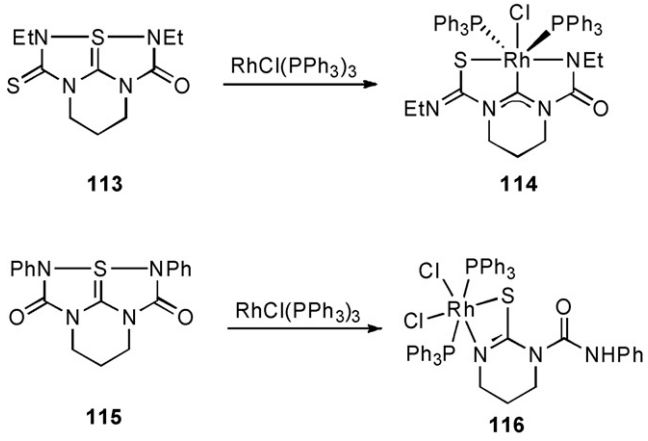

Scheme 22. Reactivity of carbonyl substituted tetraazapentalenes **113** and **115**.

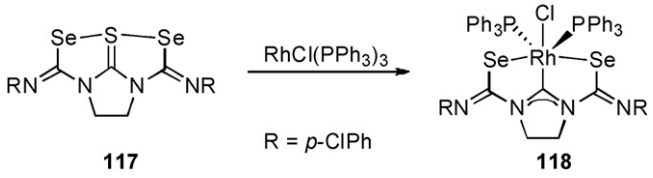

Scheme 23. Synthesis of (Se–C–Se)RhCl(PPh$_3$)$_2$ complex **118**.

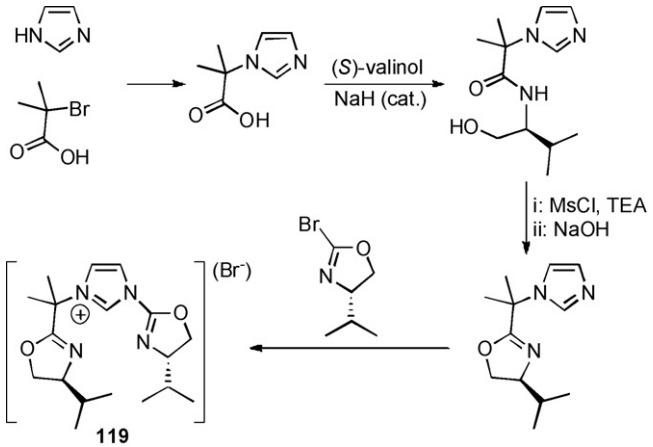

Scheme 24. Synthesis of the (ox)^CH–(ox) proligand **119**.

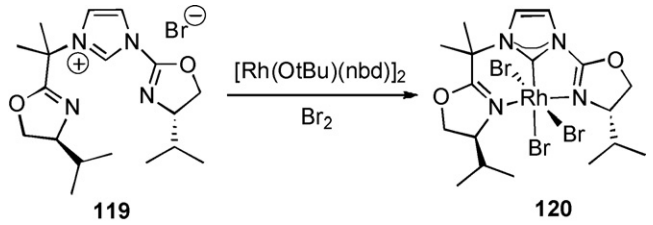

Scheme 25. Formation of (ox)^CH–(ox)RhBr$_3$ complex **120**.

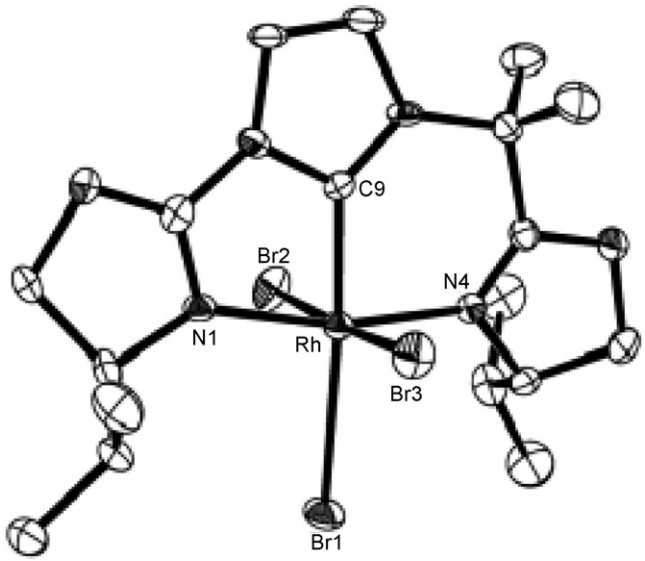

Fig. 35. The structure of complex **120** [46].

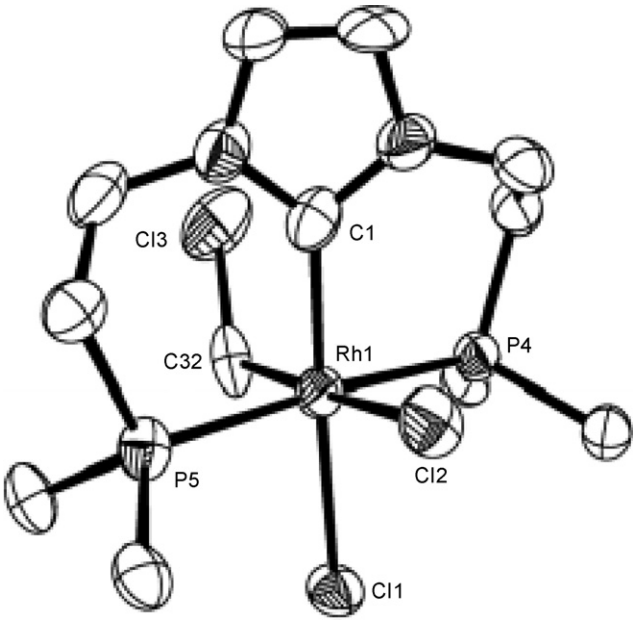

Fig. 36. The structure of (P∼C∼P)$RhCl_2(CH_2Cl)$ **123**; Ph groups except *ipso* carbons omitted for clarity [81].

metal with meridionally coordinating tridentate ligand and three bromide ions (Fig. 35). The Rh–C_{NHC} bond length of 1.900(4) Å is shorter than the previously reported Rh(III)–C_{NHC} bond length (1.930(15) Å) which could be ascribed to the structural requirements of the ligand. The ^{13}C NMR signal for the C_{NHC} was observed at 177.5 ppm.

The only (P∼C∼P) pincer complexes of Rh were reported by Lee and co-workers [81]. They were synthesised from the corresponding silver complex **69** by the reaction with either $[RhCl(CO)_2]_2$ or $[RhCl(COD)]_2$ (Scheme 26).

The reaction with $[RhCl(CO)_2]_2$ formed a five coordinate Rh(I) complex assigned as **121**. Although the flexibility of the ligand accommodates either meridional or facial coordination, the presence of only one doublet in the ^{31}P NMR spectrum was taken as evidence for the adoption of meridional geometry. No structural characterisation was possible and so the geometry remains uncertain.

The reaction with $[RhCl(COD)]_2$ in DCM did not afford the expected square planar Rh(I) compound, but rather an octahedral Rh(III) compound (**123**) formed by oxidative addition of the Cl–CH_2Cl bond to the intermediate **122**. The product was structurally characterised, showing the meridionally coordinating pincer ligand with two *cis* chloride ions and one chloromethyl ligand (Fig. 36).

When the reaction of **69** with $[RhCl(COD)]_2$ was carried out in DMF at 60 °C, a different Rh(III) product was obtained. The (P∼C∼P)$RhCl_3$ compound **124** was isolated in 70% yield. The ^{31}P NMR spectrum indicates the meridional coordination mode of the ligand. Structural characterisation confirmed the meridional geometry of the ligand, with three chloride ions completing

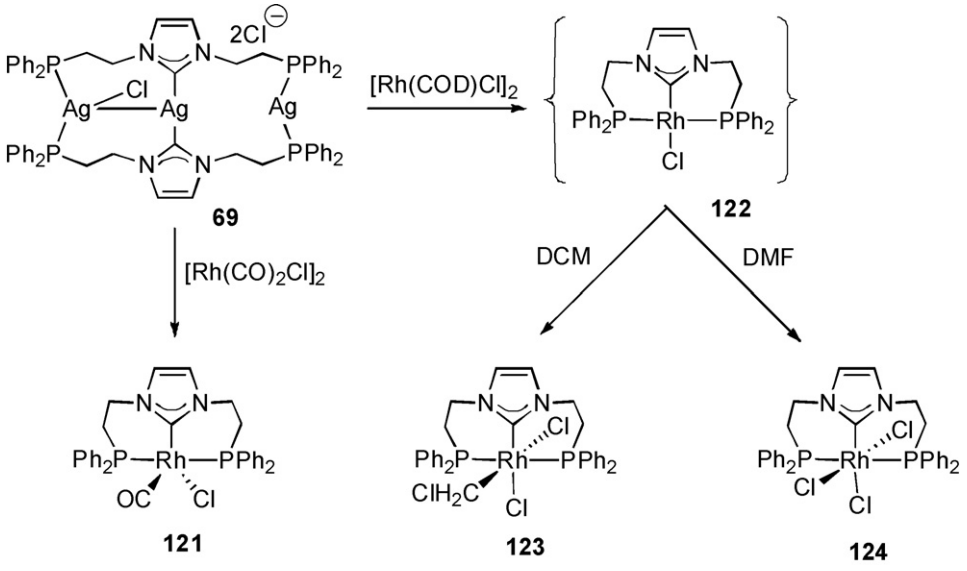

Scheme 26. Synthesis of rhodium complexes bearing the P∼C∼P ligand.

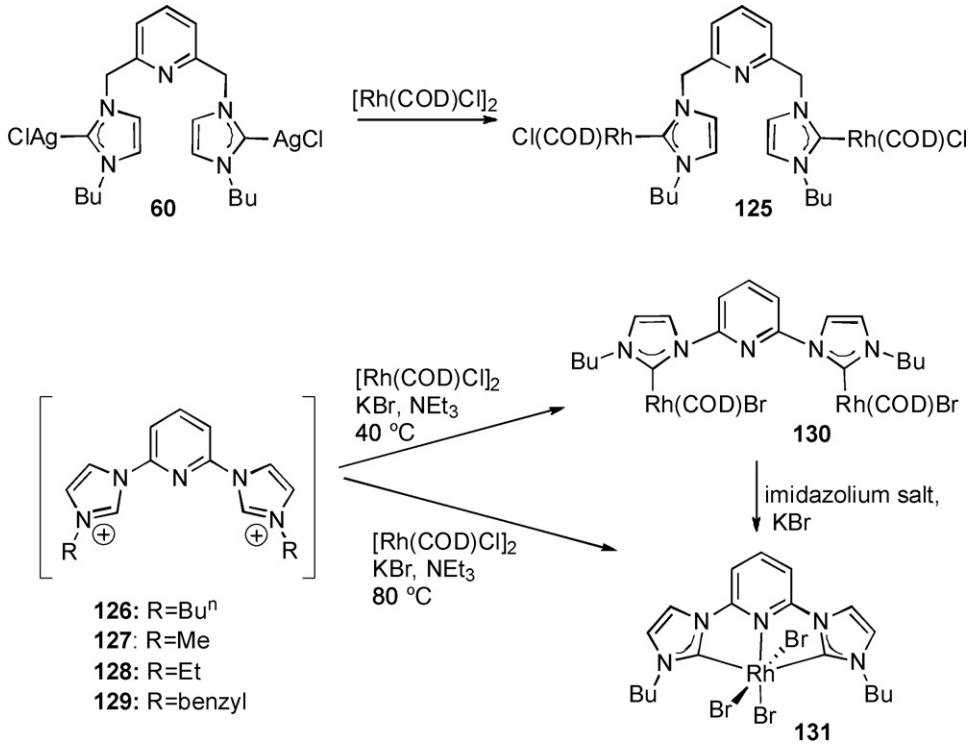

Scheme 27. Synthesis of mononuclear and dinuclear (C–N–C)Rh complexes.

the coordination sphere. It is thought the product was formed by oxidative degradation in the presence of AgCl, a process also observed with ruthenium(II) compounds [66]. The Rh–C_{NHC} bond lengths of 2.008(9) Å (**123**) and 2.003(7) Å (**124**) are within the range of known Rh(III)–C_{NHC} bond lengths. The ^{13}C NMR signals for the C_{NHC} were not observed.

The attempted synthesis of a (C^N^C)RhCl pincer *via* transmetallation from the silver complex **60** with $[Rh(COD)Cl]_2$ was attempted by Youngs and co-workers [43]. However, the isolated product was not the pincer complex but rather the dinuclear bis(rhodium) species **125**. An analogous reaction reported by Peris using imidazolium salt **126**, KBr and base rather than the silver transmetallation route also resulted in the formation of the bis(rhodium) complex **130**. Further reaction of the dimer with another equivalent of the imidazolium salt, KBr and base furnished the desired pincer complex **131**. The butyl analogue **131** was also synthesised directly by heating the imidazolium salt **126** with $[Rh(COD)Cl]_2$ (Scheme 27) [82].

Complex **131** was structurally characterised, confirming a six coordinate octahedral Rh(III) species (Fig. 37); structural characterisation of the dimeric complexes **125** and **130** was also gained. Complex **131** turned out to be a 50:50 mixture of the (C–N–C)$RhBr_3$ complex and (C–N–C)$RhBr_2Cl$ with the chloride ion *trans* to the pyridine nitrogen. The Rh–C_{NHC} bond lengths of 2.000(12) and 2.009(13) Å (**125**) and 2.029(11) and 1.948(11) Å (**130**) are within the range of known Rh(I)–C_{NHC} bonds (1.914(3)–2.102(5) Å) [83,84]. The Rh(III)–C_{NHC} bond lengths of 2.045(5) and 2.055(5) Å are also within the known range of Rh(III)–C_{NHC} distances. The ^{13}C NMR signals are found at 183.0 ppm (**125**), 184.8 ppm (**130**) and 177.5 ppm (**131**).

Imidazolium salt **126**, with PF_6^- counterions, as well as the ethyl (**128**) and benzyl (**129**) analogues, were reacted with $[Rh(CO)_2(OAc)]_2$ to form the cationic Rh(I) pincers **132–134**. The dimeric bis(rhodium) species were not observed and all reactions cleanly formed the Rh(I) pincer compound.

The Rh(I) pincer undergoes oxidative addition of MeI to form octahedral Rh(III) pincer complexes **135–137** (Scheme 28). No

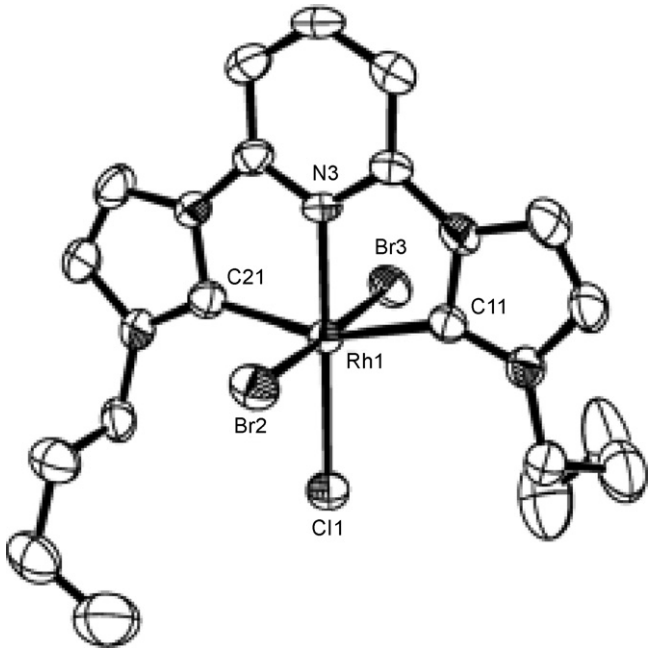

Fig. 37. The structure of (C–N–C)$RhBr_3$ pincer, showing the (C–N–C)$RhBr_2Cl$ [82] orientation.

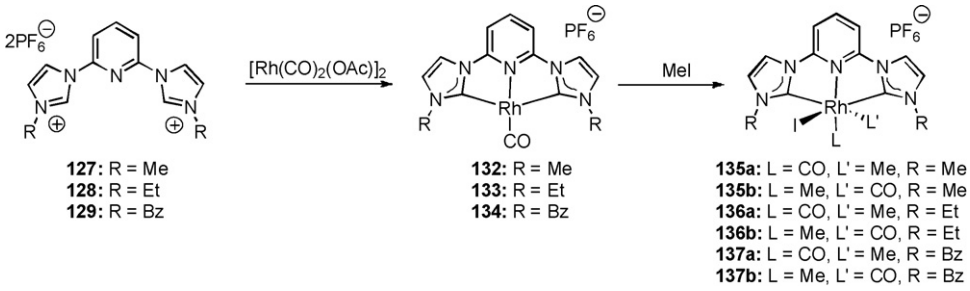

Scheme 28. Synthesis and reactivity of $[(C–N–C)Rh(CO)]^+(PF_6)_2$ complexes **132**–**134**.

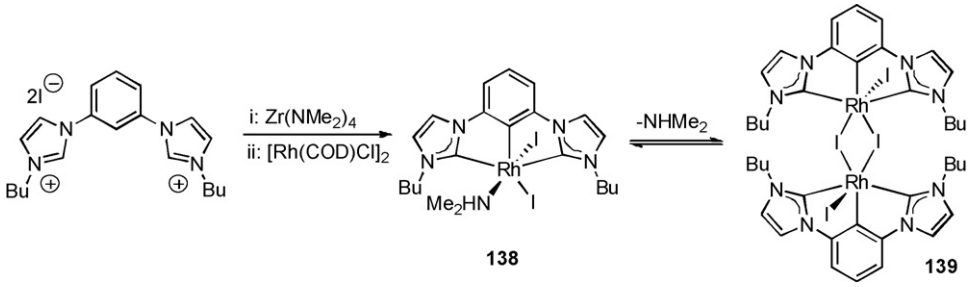

Scheme 29. Synthesis and reactivity of the $(C–C–C)RhI_2(NHMe_2)$ complex **138**.

structural characterisation or $^{13}C\{^1H\}$ NMR spectroscopy data were gathered, although the presence of two Me isomers in an 11:1 ratio (^1H NMR spectroscopy) and three νCO bands in the IR spectrum indicate the presence of at least two geometric isomers for each Rh(III) complex and a third, unknown, species. Kinetic studies on the oxidative addition reaction found that the rate was first order with respect to MeI and the Rh(I) complex, hence second order overall.

The only (C–C–C) pincer complex of rhodium was synthesised by Hollis and co-workers [85]. Transmetallation of the $(C–C–C)Zr(NMe_2)I_2$ complex **54** with $[Rh(COD)Cl]_2$ in a 1:1 ratio of ligand:Rh resulted in a 50% conversion to **138**, with 50% of the Zr complex remaining unreacted. However, a 1:2 ratio of ligand:Rh resulted in complete conversion to **138** (Scheme 29). Attempts to grow crystals of **138** *via* slow diffusion resulted in loss of $HNMe_2$, forming the iodide-bridged dimer **139**. This was structurally characterised (Fig. 38), showing Rh–C_{NHC} bond lengths of 2.063(4) and 2.061(4) Å which are within the range of known Rh(III)–C_{NHC} bonds. Attempts to form the Rh(I) pincer via reaction of the free carbene with $[Rh(COD)Cl]_2$ only resulted in the formation of a dimeric bis(rhodium) species, as seen by Youngs and Peris [37,43,82].

5.3. Catalytic reactions

The cobalt pincer complexes **104** and **107** were tested for catalytic activity for olefin polymerisation, but no activity was seen despite the use of a large excess (500–1000 equiv.) of MAO.

Complex **131** was tested as a catalyst in the transfer hydrogenation of ketones. Although it proved poor at room temperature, when heated to 80 °C it exhibited good activity. The best activity was seen with benzophenone as substrate, (0.006 mol% catalyst, 24 h, TON = 10,580). Reduction of the reaction time to 7 and 3 h dropped the TON to 6450 and 3636, respectively. Similar activity was seen with acetophenone as substrate (0.006 mol% catalyst, 6 h).

Non-pincer complex **130** exhibited good activity for the hydrosilylation of alkynes, although the *E*/*Z*/*α* product selectivity was not particularly notable. However, for certain substrates, long reaction times resulted in *E*/*Z* isomerisation competing with the hydrosilylation, leading to the thermodynamically more stable *E* isomer [82].

The $(P{\sim}C{\sim}P)RhCl_2(CH_2Cl)$ complex **123** was used to optimise conditions for the hydrosilylation experiments carried out by Lee and co-workers [81]. In common with the findings of Peris, longer reaction times increased the *E*/*Z* ratio. Bulky groups on the silane ($HSiMe_2{}^tBu$) resulted in lower stereoselectivity.

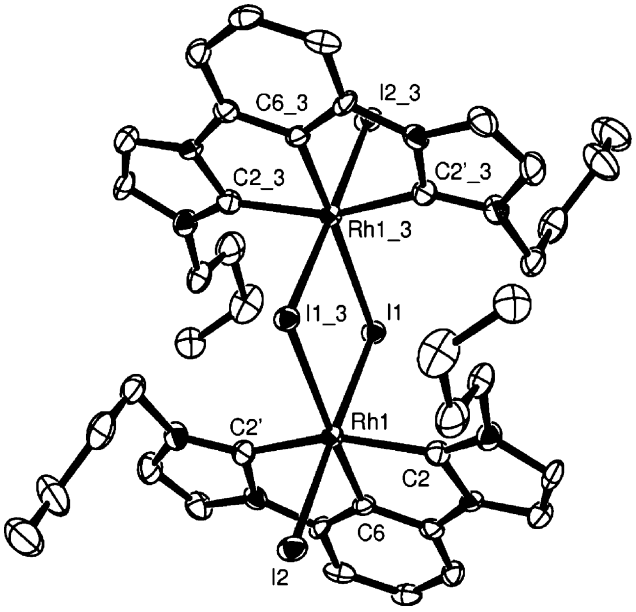

Fig. 38. The structure of Rh(III) iodide-bridged species **139** [85].

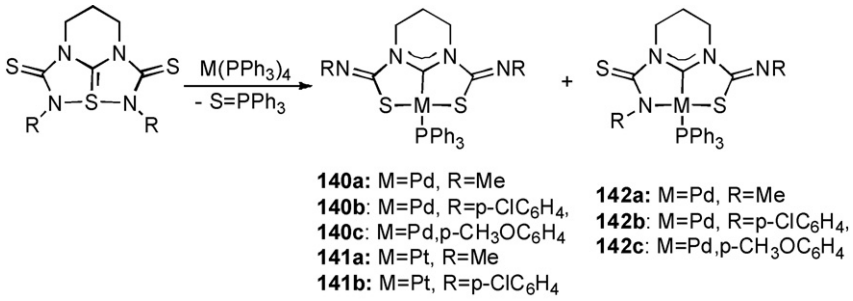

Scheme 30. Synthesis of $(S^{-}–C–S^{-})M(PPh_3)$ and $(N^{-}–C–S^{-})M(PPh_3)$ complexes **140**–**142**.

Complexes **121** and **124** were also tested in the reaction of phenylacetylene with $HSiMe_2Ph$, but showed reduced stereoselectivity for the *E* product over the *α* isomer than **123**. However, when Et_3SiH was used instead of $HSiMe_2Ph$, complex **121** proved to be the most stereoselective catalyst with no *Z* isomer and 82:18 *E*:*α* ratio.

The $(C–C–C)RhI_2(HNMe_2)$ complex **138** was tested as a hydrosilylation catalyst (2–3.5 mol% catalyst, 1:1.1 substrate:silane ($HSiMe_2Ph$), $CDCl_3$ at 80 °C). The best activity was found with phenylacetylene. The selectivity observed with this catalyst is the opposite seen with the (C–N–C) and (P∼C∼P) systems. Increasing the reaction time to 12 h had no effect on the *E*:*Z* ratio. In general, terminal alkynes favoured the *Z* isomer, whereas internal alkynes favoured the *E* product [37]. Additives such as LiCl, water and Bu_4NBr markedly reduced the *E*:*Z* selectivity for terminal alkynes, although internal alkynes were unaffected.

6. Group 10 metal complexes

The majority of linear rigid tridentate complexes with group 10 metals incorporate Pd(II). There are no examples of isolated and characterised Pd(0) complexes even though they have been postulated as intermediates in homogeneous catalytic reactions. The first heteroatom functionalised 'pincer' complexes of Pd(II) and Pt(II) were isolated by the reaction of trithiaazapentalenes with $M(PPh_3)_4$ (M = Pd, Pt; Scheme 30). The structures determined by X-ray crystallography unequivocally establish the metal–carbene functionality [74,79,86].

The metallapentalene framework features planar structures with one metal–carbene and two metal–sulfur bonds. Even though isomeric products in which the metal is coordinated by the N atoms in addition to the carbene carbon have been detected by ^1H NMR spectroscopy, they isomerised to the thermodynamically stable structures with M–S coordination. The platinum

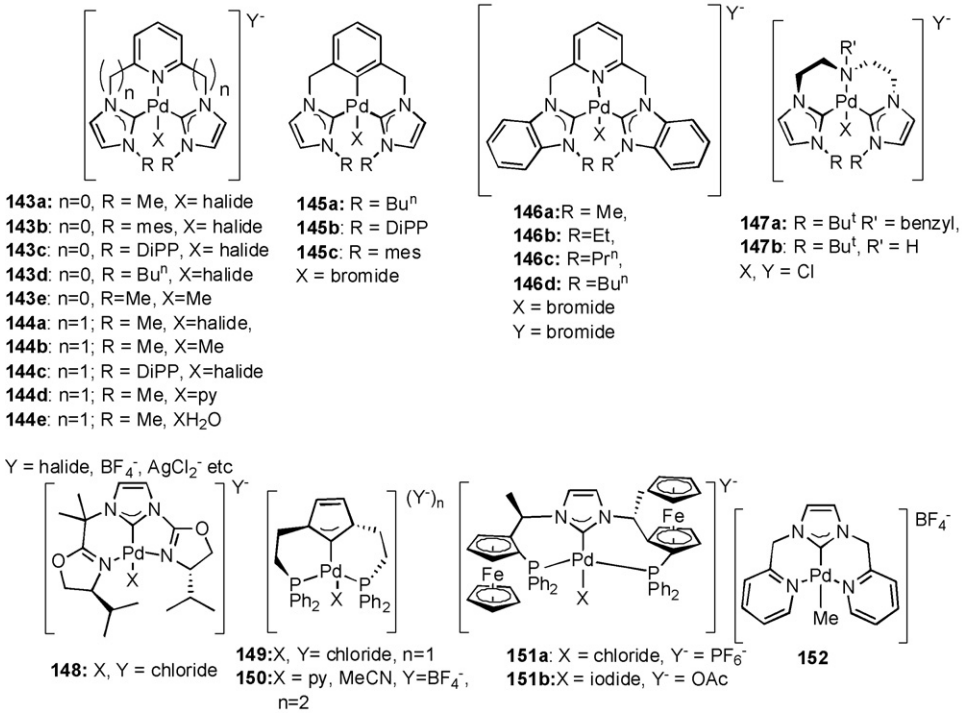

Fig. 39. Palladium complexes with the rigid tridentate ligands discussed in this paper.

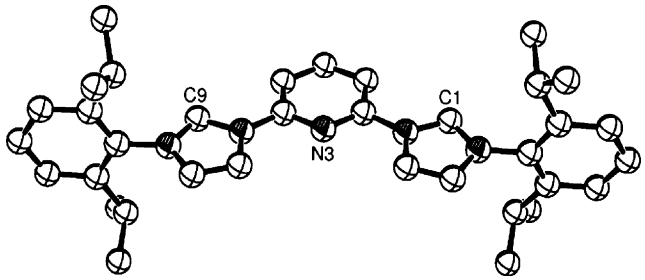

Fig. 40. The structure of the free ligand **36** [4].

complex reported in this work is, until now, the only example of a platinum complex with a rigid tridentate ligand containing carbene donors.

6.1. Palladium

Currently, the most thoroughly studied palladium(II) pincer complexes are based on the 2,6-(dicarbene)-pyridine (C–N–C) and α,α′-(dicarbene)-2,6-lutidine (C^N^C) systems (Fig. 39).

The proligand salts (CH–N–CH)Br_2, (CH^N^CH)Br_2 and (BzCH^N^CHBz)Br_2 have been obtained easily and in synthetically useful quantities by the quaternisation of alkyl- and aryl-imidazoles or -benzimidazoles with 2,6-dibromopyridines or 2,6-bis-(bromomethyl)-pyridines, respectively [9,10,87,88]. The reactions are usually carried out at high temperatures (120–150 °C) in the absence of solvents. In many cases, the (C–N–C) ligands have been isolated as air sensitive, thermally stable solids by deprotonation of the proligand salts with various bases, preferentially $KN(SiMe_3)_2$ [4], and structurally characterised (Fig. 40).

The isolation of free (C^N^C) and (BzC^N^CBz) ligands has not been successful so far, possibly due to unselective deprotonation of the proligand and the limited thermal stability of the product. However, (C^N^C) ligands have been generated *in situ* by deprotonation methodology and used for further reactions with metal precursors. Quaternisation of α,α′-dibromo-1,3-xylene and α,α′-dibromo-2-bromo-1,3-xylene with alkyl- or aryl-imidazoles leads to the imidazolium salts (CH^CH^CH)Br_2 and (CH^CBr^CH)Br_2, respectively, which serve as precursors to carbene complexes by metallation of the aromatic ring under various conditions [89,90].

Ionic palladium complexes of the type [Pd(C–N–C)X]Y and [Pd(C^N^C)X]Y were prepared by direct reaction of the corresponding bis-imidazolium salts with $Pd(OAc)_2$ in DMSO at 160 °C [9], transmetallation of the silver carbene complexes with $Pd(COD)Cl_2$ [10], $Pd(MeCN)_2Cl_2$ and Pd(COD)MeCl [42,91], or by the substitution of labile COD in $Pd(COD)Cl_2$ by the isolated (C–N–C) [89]. The cations $[Pd(C–N–C)X]^+$ X = Cl, Br, and $[Pd(C^N^C)X]^+$ (X = Cl, Br, Me) were isolated in combination with various anions (Y^-), the nature of which (halide, $[Ag(halide)_2]^-$ or BF_4^-) was dependent on the synthetic method used. Additional derivatives $[Pd(C^N^C)X]^+Y^-$ and $[Pd(C^N^C)L]^+Y^-$ (L = H_2O, pyridine, Y = I^-, toluenesulfonate, BF_4^-, etc.) were prepared by anion metathesis reactions with AgY in the presence of L [92]. Various substituents on N3

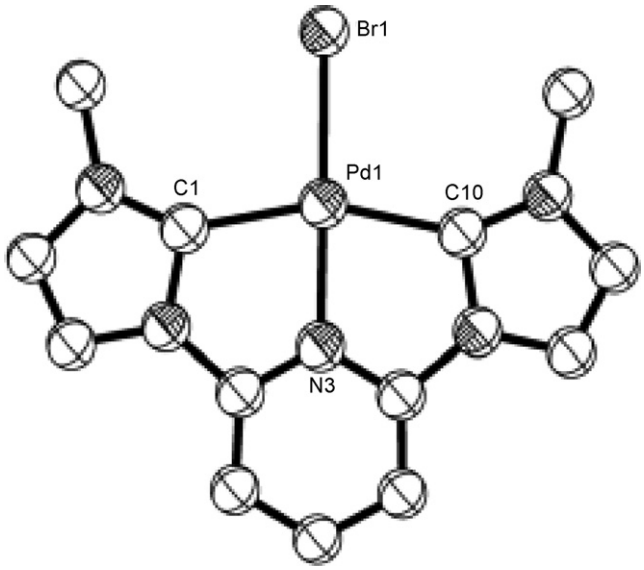

Fig. 41. The cation $[(C–N–C)PdCl]^+$ **143a** [9].

of the carbene heterocycle (Me [9,42] ^{n}Bu [43,90], mesityl, 2,6-D*i*PP [10,89]) have also been introduced in order to increase the solubility, study the dynamic behaviour of the complexes in solution, modify the sterics at the metal and influence the catalytic activity. The structures of the complexes feature a planar 2,6-(dicarbene)-pyridine cation, (Fig. 41) or helical α,α′-(dicarbene)-2,6-lutidine cation (Fig. 42).

The common feature of all reported structures is the almost square planar geometry of the Pd centre. The Pd–C_{NHC} bond lengths are within the expected range (ca. 1.98–2.05 Å). In the pyridine-based systems (**143a–d**) the coordination plane is virtually co-planar with the plane defined by the heterocyclic rings of the 'pincer', while in the lutidine systems (**144a–e**) the square planar geometry at Pd is attained by a twist of the coordination

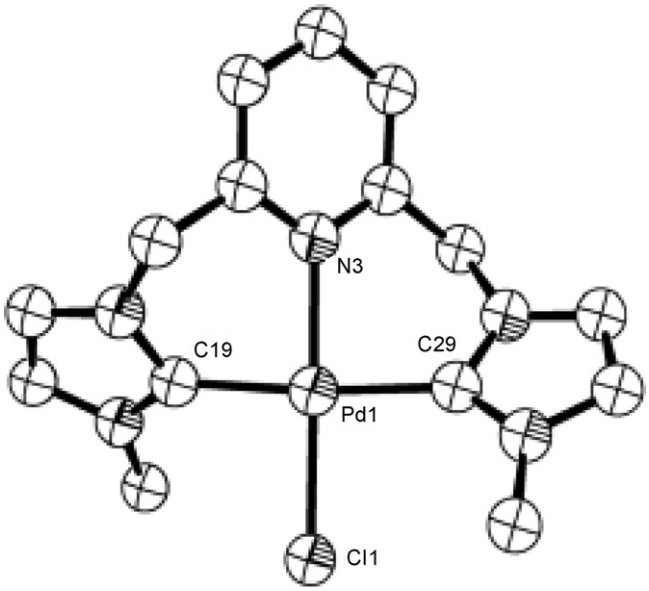

Fig. 42. The cation $[(C^N^C)PdCl]^+$ **144c**; Ar groups bar *ipso* carbons omitted for clarity [10].

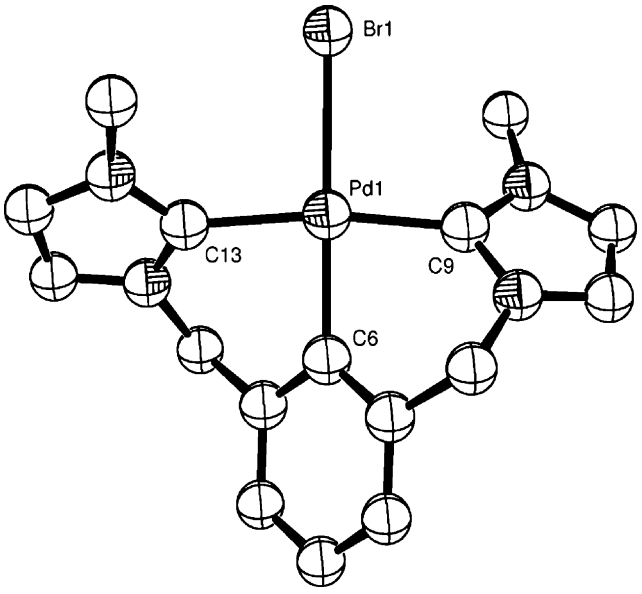

Fig. 43. The structure of the complex **145a** [90].

plane relative to the plane of the lutidine ring. The helical structures created in this way exhibit chirality, which was confirmed by the addition of chiral shift reagents resulting in the selective shift of the ^{1}H NMR signals associated with one of the enantiomers present in solution (R = D*i*PP) [10]. The thermodynamic parameters for the interconversion of the two enantiomeric conformers (atropoisomerisation) of an analogue (R = Me) were measured by line shape analysis of the ^{1}H NMR spectra within a temperature range and are consistent with an intramolecular process ($\Delta S^{\ddagger} = 0$) [92].

Palladium 'pincer' complexes with an anionic aromatic carbon bridgehead (C^C^C) instead of the neutral pyridine group have also been prepared by either the cyclometallation of the 1,3-xylyl-bis-imidazolium salts (CH^CH^CH)Br_2 with $Pd(OAc)_2$ and NaOAc in DMAc at 160 °C, or by the reaction of $Pd_2(dba)_3$ with 2-bromo-l,3-(α,α′-bis-imidazolium)-xylene (CH^CBr^CH)Br_2. The neutral Pd(C^C^C)Br complexes obtained feature helical chiral structures with square planar coordination geometry at Pd (Fig. 43) [89,90].

A detailed study of the atropoisomerisation (Scheme 31) of the [Pd(C^N^C)X]Y complexes by ^{1}H NMR spectroscopy showed a dependence of the activation parameters on the nature of the counterion Y^- occupying the outer coordination sphere of the metal. Interconversions were faster with strongly coordinating and nucleophilic Y^- (e.g. I^-, Br^-) and retarded by weakly nucleophilic Y^- (e.g. toluenesulfonate, etc.) and in the system [Pd(C^C^C)Br]. The observed differences were accounted for by the postulation of two alternative mechanisms operating during the isomerisation. The first, which is dominant in the [Pd(C^N^C)X]Y complexes with Y^- being a weakly nucleophilic anion and in the [Pd(C^C^C)Br] complexes, the fluxional process takes place in two steps involving a non-synchronous move of the NHC groups through the square plane *via* an unsymmetrical cationic four coordinate intermediate. In the second mechanism, which is dominant in [Pd(C^N^C)X]Y complexes with Y^- a strongly nucleophilic anion, a reversible displacement of the pyridine donor of the 'pincer' by the nucleophilic anion Y^- forms a neutral *trans*-biscarbene dihalide complex, which undergoes fast conformational change and atropoisomerisation [92]. The two mechanistic models were supported by computational methods and may describe possible pathways leading to coordinatively unsaturated species in catalytic reactions. The rigid coordination sphere provided by the 'pincer' (C^N^C) and (C–N–C) ligands allowed the investigation of elementary organometallic reactions in a well-defined *N*-heterocyclic carbene coordination environment.

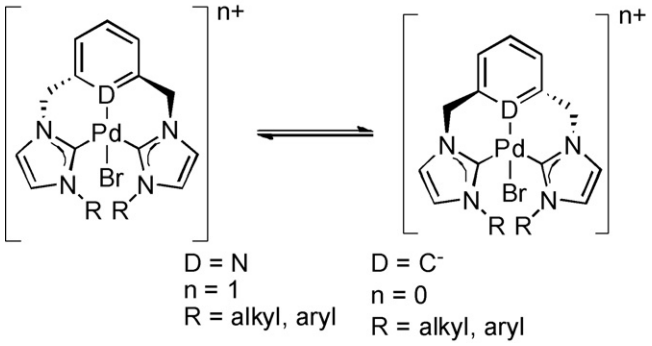

Scheme 31. Atropoisomerisation of the complexes **144** and **145**.

Thermolysis of the [Pd(C^N^C)Me]$^+$(BF_4) (**144b**) and [Pd(C–N–C)Me]$^+$(BF_4) (**143e**) (R = Me) in DMSO-d_6 was followed by the disappearance of the Pd–Me signal in the ^{1}H NMR spectra. It gave rise to 2-methyl-imidazolium substituted pyridine species resulting from the reductive elimination of 2-methyl-imidazolium and formation of Pd(0) [91]. DFT calculations supported the observed reactivity of the complexes [Pd(C^N^C)Me](BF_4) and [Pd(C–N–C)Me](BF_4), establishing a correlation of the barrier for the reductive elimination and the out-of-plane carbene twists, with increased twist angles (originating from the presence of the CH_2 linker in C^N^C and/or a bulky R on the carbene functionality) leading to lower elimination barriers. These results are in agreement with previously published experimental and theoretical work [93]. The reaction of the isolated (C–N–C) 'pincer' ligand (R = 2,6-D*i*PP) with Pd(tmeda)(CH_3)$_2$, gave a complex (Figs. 44 and 45) which constitutes the first example of migratory insertion of an alkyl group to the carbene carbon of an *N*-heterocyclic carbene.

All Pd–C bond lengths in this complex are very similar. DFT studies established a plausible mechanism for the complex formation involving substitution of the labile tmeda by the 'pincer' ligand, forming a high energy five coordi-

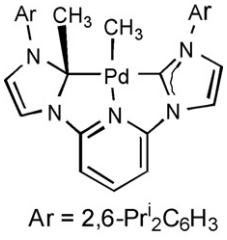

Fig. 44. Diagram showing the Me migration to the C_{NHC}.

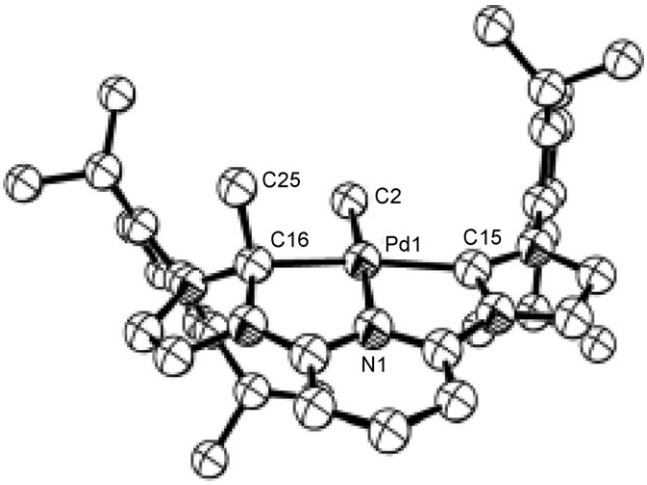

Fig. 45. The structure of the migratory insertion product [94].

nate (C–N–C)Pd$(CH_3)_2$ in which a methyl group undergoes migration to the C_{NHC} and formation of the observed product [94]. Other NHC-containing rigid tridentate ligands have been reported in the literature (see Fig. 39) and their palladium complexes studied by various methods. The benzimidazol-2-ylidene ligand analogues of (C^N^C) i.e. (BzC^N^BzC) with a variety of alkyl substitution at the benzimidazole nitrogen (R = Me, Et, Pr^n, Bu^n) were complexed to palladium by the reaction of the benzimidazolium bromides with $Pd(OAc)_2$ in DMSO (complexes **146a–d**) [88]. The benzimidazolium proligands were synthesised by quaternisation reactions of the substituted pyridines with substituted benzimidazoles. The effect of the change of the NHC-type on the Pd–C_{NHC} bond length is minimal. The complexes adopt a distorted square planar chiral structure which undergo intramolecular atropoisomerisation with activation parameters similar to the (C^N^C) species (Fig. 46).

The more flexible tridentate dicarbene amine proligand (CH∼NR′∼CH)Cl_2 was also prepared by the quaternisation of the protected *N*-benzylated bis-(2-chloroethyl)amine with substituted imidazoles. After debenzylation it was used for the synthesis of dicarbene-amine palladium complexes. The synthetic method of choice leading to $[Pd(C{\sim}NH{\sim}C)Cl]^+Cl^-$

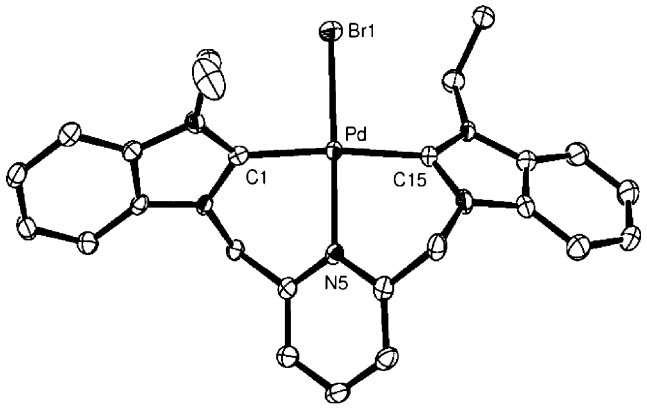

Fig. 46. The cation of the complex **146b** [88].

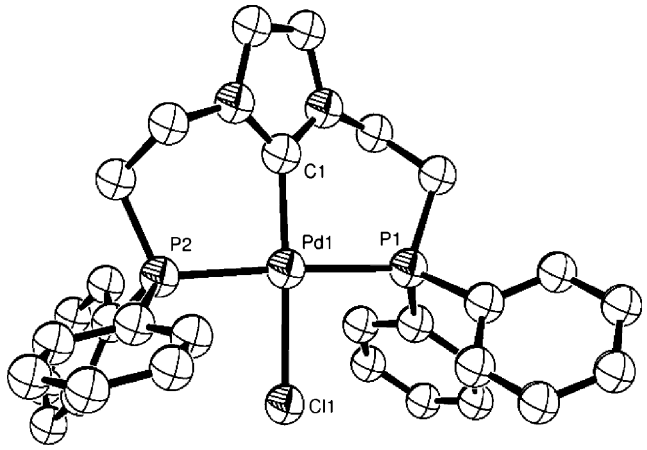

Fig. 47. The cation of complex **149** [47].

(**147b**) involved transmetallation of the silver carbene complex with $PdCl_2(MeCN)_2$. The Pd(C∼NH∼C) cations adopt fluxional helical structures with square planar palladium centres as described above [45]. Interestingly, deprotonation of the coordinated secondary amine nitrogen with NaH gave the neutral Pd(C∼N∼C)Cl, incorporating an amido functional group at the bridgehead position, which was characterised by analytical and spectroscopic methods. Amido complexes of the late transition metals are rare and usually stabilised by incorporation of the amido group in chelate structures.

The Pd complex **148** with the ox^C–ox ligand was synthesised by transmetallation from the analogous silver carbene to $Pd(COD)Cl_2$ [46].

The (N^C^N) ligand has been used for the synthesis of cationic Pd(II) methyls, showing improved stability towards reductive elimination of 2-methylimidazolium salts by virtue of the *trans*-arrangement of the NHC and the methyl functionalities which are subject to the reductive elimination [42].

The reaction of the (P^CH^P)Cl ligand with $PdCl_2$ gave the complex **149** [47]. The same species can be obtained by transmetallation from the silver complex to $PdCl_2$. The structure of the cation (Fig. 47) shows a square planar palladium centre and the plane of the imidazole ring twisted from the coordination plane giving an overall chiral structure. In solution, fluxionality is observed, which is ascribed to conformational changes leading to enantiomeric interconversion. Abstraction of the coordinated chloride ion in the cation $[(P{\sim}C{\sim}P)PdCl]^+$ with $AgBF_4$ in pyridine or acetonitrile gave complexes $[(P^C^P)PdL]^+(BF_4^-)_2$, L = acetonitrile, pyridine (**150**) which maintain the structural and dynamic features of the starting material.

The (FcP^C^FcP) ligand was introduced to Pd by either generation of the free carbene *in situ* from the imidazolium iodide and $NaOBu^t$ and trapping it with $Pd(COD)Cl_2$ in the presence of $TlPF_6$ (**151a**) or, more conveniently, by the reaction of the imidazolium iodide with palladium acetate in THF (**151b**) [95]. The complex maintains the C_2 symmetry in solution as demonstrated by NMR spectroscopy; however, in the solid state a less symmetric structure is observed (Fig. 48) due to the orientation of the phenyl rings on the phosphorus atoms and the ferrocenyl backbones. The observed symmetric structure in solution may

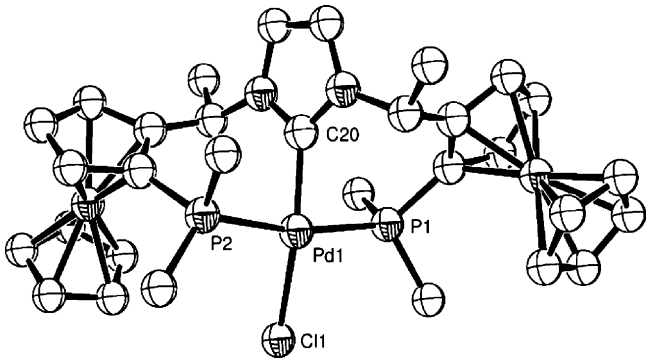

Fig. 48. The cation of the complex **151a**; Ph groups bar *ipso* carbons omitted for clarity [100].

be due to fast averaging of non-symmetric structures similar to the one observed in the solid state.

6.1.1. Catalytic studies of the Pd species

Complexes of the type **143**, **144**, **146** and **149** have been used as catalysts in the Heck olefination reaction. The studies are limited to two olefinic substrates (styrene and *n*-butyl acrylates) and cover a range of aryl halides exhibiting varied activity. Initial reports using the complexes **143** and **144** [9,10,90] showed that activity is maintained at higher temperatures (120–140 °C) in dimethylformamide, dimethylacetamide or *N*-methylpyrrolidone solvents. The bases of choice are NaOAc, triethylamine or Na_2CO_3. The activities of the catalysts are high for aryl iodides and bromides at low catalyst loading. Only activated aryl chlorides are reactive at higher catalyst loading (5 mol%) and sometimes in the presence of Bu^n_4Br. Less bulky substituents on the NHC nitrogen atom give more reactive systems. Comparison of the activities of the C^N^C and C^C^C complexes indicates higher activity for the former ligand system. Comparable catalytic results were later reported for complexes of the type **146**, indicating that the nature of the NHC is not so important in determining the activity of the 'pincer' catalysts. The exact mechanism and the nature of the catalytic species in these reactions is not clear. Recent proposals on the nature of the catalytic species in non-NHC pincer complexes support the generation of Pd nanoparticles under the reaction conditions [96], however, the evidence is far from conclusive that nanoparticles are also involved in the NHC-pincer systems which, under non-catalytic conditions, show remarkable stability. In addition, the reactivity towards aryl chlorides points to the presence of homogeneous catalysts in operation. Complexes **149** have also been studied as catalysts in the Heck and Suzuki reaction with more encouraging results in the former. The complexes are active with aryl bromides and iodides, and some low activity for the activated aryl chlorides has been observed [47]. High activities for the Heck reaction of bromoacetophenone with butyl acrylate have been observed with complex **152** and has been ascribed to the blocking of catalyst decomposition by the pyridine wingtips and possible hemilability.

More work is desirable in elucidating the nature of the catalytic species in these reactions and the development of new catalysts capable of catalysing the reaction of non-activated or deactivated aryl chlorides.

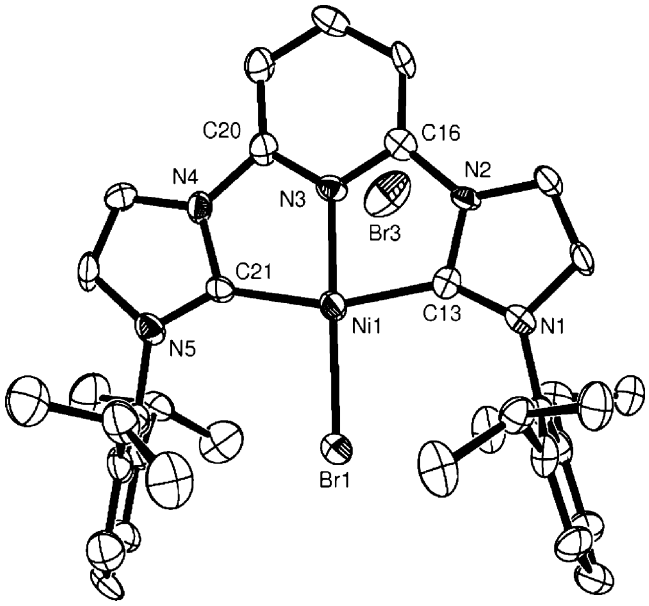

Fig. 49. The cation ((C–N–C)NiBr)(Br) [97].

6.2. Nickel complexes

Even though nickel *N*-heterocyclic carbene complexes are common, there is only one example with the 'pincer' ligand, i.e. the [Ni(C–N–C)Br]Br prepared by the reaction of **36** with $NiBr_2$(dme) [97]. The metal is in a square planar environment (Fig. 49) with short Ni–C_{NHC} (1.923 Å) bond lengths.

The reactivity of this complex has not yet been reported.

7. Conclusions—future outlook

From the work discussed above, it is clear that the tridentate 'pincer'-type ligands bearing NHC donor groups have been responsible for the development of some exciting new areas in coordination and organometallic chemistry with possible applications in catalysis. The use of the existing ligand designs in early transition metals and electrophilic high oxidation states is still not well studied. Applications of a bioinorganic nature are also rare. The synthesis of new linear rigid tridentate ligand systems with modified topologies, functional groups (including different types of singlet carbene donors), chirality and hemilability will certainly assist future developments in all these areas.

The understanding of the organometallic chemistry in metal coordination spheres involving NHC ligands will also help the design of new catalysts. We are certain that exciting work in these areas will appear in the near future.

References

[1] R.H. Crabtree, J. Organomet. Chem. 690 (2005) 5451.
[2] M.F. Lappert, J. Organomet. Chem. 358 (1988) 185.
[3] H.M.J. Wang, I.J.B. Lin, Organometallics 17 (1998) 972.
[4] A.A. Danopoulos, S. Winston, W.B. Motherwell, Chem. Commun. (2002) 1376.

[5] A.A. Danopoulos, S. Winston, T. Gelbrich, M.B. Hursthouse, R.P. Tooze, Chem. Commun. (2002) 482.
[6] A. Furstner, L. Krause, L. Ackermann, C.W. Lehmann, Chem. Commun. (2001) 2240.
[7] X. Hu, I. Castro-Rodriguez, K. Meyer, Organometallics 22 (2003) 3016.
[8] E. Mas-Marza, M. Poyatos, M. Sanau, E. Peris, Organometallics 23 (2004) 323.
[9] E. Peris, J.A. Loch, J. Mata, R.H. Crabtree, Chem. Commun. (2001) 201.
[10] A.A.D. Tulloch, A.A. Danopoulos, G.J. Tizzard, S.J. Coles, M.B. Hursthouse, R.S. Hay-Motherwell, W.B. Motherwell, Chem. Commun. (2001) 1270.
[11] J.C.C. Chen, I.J.B. Lin, Dalton (2000) 839.
[12] M.E. van der Boom, D. Milstein, Chem. Rev. 103 (2003) 1759.
[13] M. Albrecht, G. van Koten, Angew. Chem. Int. Ed. Engl. 40 (2001) 3750.
[14] B.C. Bailey, H. Fan, E.W. Baum, J.C. Huffman, M.-H. Baik, D.J. Mindiola, J. Am. Chem. Soc. 127 (2005) 16016.
[15] J. Campora, P. Palma, D. del Rio, E. Alvarez, Organometallics 2004 (2004) 1652.
[16] N.D. Jones, R.G. Cavell, J. Organomet. Chem. 690 (2005) 5485.
[17] R.G. Cavell, R.P.K. Babu, K. Aparna, J. Organomet. Chem. 617 (2001) 158.
[18] H. Aihara, T. Matsuo, H. Kawaguchi, Chem. Commun. (2003) 2204.
[19] S. Solé, H. Gornitzka, O. Guerret, G. Bertrand, J. Am. Chem. Soc. 120 (1998) 9100.
[20] A.W. Addison, T.N. Rao, J. Reedijk, J. van Rijn, G.C. Verschoor, J. Chem. Soc. Dalton Trans. (1984) 1349.
[21] N. Kuhn, T. Kratz, D. Blaser, R. Boese, Inorg. Chim. Acta 238 (1995) 179.
[22] P. Shukla, J.A. Johnson, D. Vidovic, A.H. Cowley, C.D. Abernethy, Chem. Commun. (2004) 360.
[23] L.P. Spencer, S. Winston, M.D. Fryzuk, Organometallics 23 (2004) 3372.
[24] L.P. Spencer, M.D. Fryzuk, J. Organomet. Chem. 690 (2005) 5788.
[25] A. Weiss, H. Pritzkow, W. Siebert, Eur. J. Inorg. Chem. (2002) 1607.
[26] M. Niehues, G. Kehr, G. Erker, B. Wibbeling, R. Frohlich, O. Blacque, H. Berke, J. Organomet. Chem. 663 (2002) 192.
[27] M. Niehues, G. Kehr, R. Frohlich, G. Erker, Z. Naturforsch. B: Chem. Sci. 58 (2003) 1005.
[28] D.S. McGuinness, V.C. Gibson, D.F. Wass, J.W. Steed, J. Am. Chem. Soc. 125 (2003) 12716.
[29] D.S. McGuinness, V.C. Gibson, J.W. Steed, Organometallics 23 (2004) 6288.
[30] D. Pugh, J.A. Wright, S. Freeman, A.A. Danopoulos, Dalton Trans. (2006) 775.
[31] A. Wacker, C.G. Yan, G. Kaltenpoth, A. Ginsberg, A.M. Arif, R.D. Ernst, H. Prtizkow, W. Siebert, J. Organomet. Chem. 641 (2002) 195.
[32] C.D. Abernethy, J.A.C. Clyburne, A.H. Cowley, R.A. Jones, J. Am. Chem. Soc. 121 (1999) 2329.
[33] J. Chai, H. Zhu, Y. Peng, P.W. Roesky, S. Singh, H.-G. Schmidt, M. Noltemeyer, Eur. J. Inorg. Chem. (2004) 2673.
[34] J. Chai, H. Zhu, K. Most, P.W. Roesky, D. Vidovic, H.-G. Schmidt, M. Noltemeyer, Eur. J. Inorg. Chem. (2003) 4332.
[35] W.J. Evans, S.A. Kozimor, J.W. Ziller, Polyhedron 23 (2004) 2689.
[36] P.L. Arnold, A.J. Blake, C. Wilson, Chem. Eur. J. 11 (2005) 6095.
[37] G.T.S. Andavan, E.B. Bauer, C.S. Letko, T.K. Hollis, F.S. Tham, J. Organomet. Chem. 690 (2005) 5938.
[38] V.C. Gibson, S.K. Spitzmesser, Chem. Rev. 103 (2003) 283.
[39] G.J.P. Britovsek, V.C. Gibson, D.F. Wass, Angew. Chem. Int. Ed. Engl. 38 (1999) 428.
[40] D. Hollmann, A.R. Kennedy, M.D. Spicer, T. Ramnial, J.A.C. Clyburne, C.D. Abernethy, J. Organomet. Chem. 690 (2005) 5346.
[41] J.C. Garrison, W.J. Youngs, Chem. Rev. 105 (2005) 3978.
[42] D.J. Nielsen, K.J. Cavell, B.W. Skelton, A.H. White, Inorg. Chim. Acta 327 (2002) 116.
[43] R.S. Simons, P. Custer, C.A. Tessier, W.J. Youngs, Organometallics 22 (2003) 1979.
[44] A. Caballero, E. Diez-Barra, F.A. Jalon, S. Merino, A.M. Rodriguez, J. Tejeda, J. Organomet. Chem. 627 (2001) 263.
[45] R.E. Douthwaite, J. Houghton, B.M. Kariuki, Chem. Commun. (2004) 698.
[46] N. Schneider, V. Cesar, S. Bellemin-Laponnazand, L.H. Gade, Organometallics 24 (2005) 4886.
[47] H.M. Lee, J.Y. Zeng, C.H. Hu, M.T. Lee, Inorg. Chem. 43 (2004) 6822.
[48] P.L. Arnold, A.C. Scarisbrick, A.J. Blake, C. Wilson, Chem. Commun. (2001) 2340.
[49] V.J. Catalano, M.A. Malwitz, Inorg. Chem. 42 (2003) 5483.
[50] A.A.D. Tulloch, A.A. Danopoulos, S. Winston, S. Kleinhenz, G. Eastham, Dalton (2000) 4499.
[51] J.C. Garrison, A.T. Claire, J.Y. Wiley, J. Organomet. Chem. 690 (2005) 6008.
[52] P.L. Chiu, H.M. Lee, Organometallics 24 (2005) 1692.
[53] J.C. Garrison, R.S. Simons, W.G. Kofron, C.A. Tessier, W.A. Youngs, Chem. Commun. (2001) 1780.
[54] S. Gischig, A. Togni, Organometallics 24 (2005) 203.
[55] I.S. Edworthy, M. Rodden, S.A. Mungur, K.M. Davis, A.J. Blake, C. Wilson, M. Schröder, P.L. Arnold, J. Organomet. Chem. 690 (2005) 5710.
[56] A.A. Danopoulos, unpublished data.
[57] A.A.D. Tulloch, A.A. Danopoulos, S. Kleinhenz, M.E. Light, M.B. Hursthouse, G. Eastham, Organometallics 20 (2001) 2027.
[58] A.A. Danopoulos, N. Tsoureas, J.A. Wright, M.E. Light, Organometallics 23 (2004) 166.
[59] L.N. Appelhans, D. Zuccaccia, A. Kovacevic, A.R. Chianese, J.R. Miecznikowski, A. Macchioni, E. Clot, O. Eisenstein, R.H. Crabtree, J. Am. Chem. Soc. 127 (2005) 16299.
[60] G. Huttner, W. Gartzke, Chem. Ber. (1972) 2714.
[61] M. Scholl, S. Ding, C.W. Lee, R.H. Grubbs, Org. Lett. 1 (1999) 953.
[62] V.M. Ho, L.A. Watson, J.C. Huffman, K.G. Caulton, New J. Chem. 27 (2003) 1446.
[63] S. Burling, M.F. Mahon, B.M. Paine, M.K. Whittlesey, J.M.J. Williams, Organometallics 23 (2004) 4537.
[64] M. Poyatos, J.A. Mata, E. Falomir, R.H. Crabtree, E. Peris, Organometallics 22 (2003) 1110.
[65] S.U. Son, K.H. Park, Y.-S. Lee, B.Y. Kim, C.H. Choi, M.S. Lah, Y.H. Jang, D.-J. Jang, Y.K. Chung, Inorg. Chem. 43 (2004) 6896.
[66] P.L. Arnold, A.C. Scarisbrick, Organometallics 23 (2004) 2519.
[67] R.B. Bedford, M. Betham, D.W. Bruce, A.A. Danopoulos, R.M. Frost, M. Hird, J. Org. Chem. 71 (2006) 1104.
[68] A.A. Danopoulos, J.A. Wright, W.B. Motherwell, S. Ellwood, Organometallics 23 (2004) 4807.
[69] D.W. Macomber, R.D. Rogers, Organometallics 4 (1985) 1485.
[70] X. Hu, I. Castro-Rodriguez, K. Meyer, J. Am. Chem. Soc. 126 (2004) 13464.
[71] E. Fooladi, B. Dalhus, M. Tilset, Dalton (2004) 3909.
[72] R.W. Simms, M.J. Drewitt, M.C. Baird, Organometallics 21 (2002) 2958.
[73] X. Hu, K. Meyer, J. Am. Chem. Soc. 126 (2004) 16322.
[74] N. Matsumura, J. Kawano, N. Fukunishi, H. Inoue, J. Am. Chem. Soc. 117 (1995) 3623.
[75] N. Matsumura, M. Tomura, S. Yoneda, K. Toriumi, Chem. Lett. (1986) 1047.
[76] W.-L. Duan, M. Shi, G.-B. Rong, Chem. Commun. (2003) 2916.
[77] N.M. Scott, R. Dorta, E.D. Stevens, A. Correa, L. Cavallo, S.P. Nolan, J. Am. Chem. Soc. 127 (2005) 3516.
[78] F. Iwasaki, M. Yasui, S. Yoshida, H. Nishiyama, S. Shimamoto, N. Matsumura, Bull. Chem. Soc. Jpn. 69 (1996) 2759.
[79] N. Manabe, M. Yasui, H. Nishiyama, S. Shimamoto, N. Matsumura, F. Iwasaki, Bull. Chem. Soc. Jpn. 69 (1996) 2771.
[80] F. Iwasaki, N. Manabe, H. Nishiyama, K. Takada, M. Yasui, M. Kusamiya, N. Matsumura, Bull. Chem. Soc. Jpn. 70 (1997) 1267.
[81] J.Y. Zeng, M.H. Hsieh, H.M. Lee, J. Organomet. Chem. 690 (2005) 5662.
[82] M. Poyatos, E. Mas-Marza, J.A. Mata, M. Sanau, E. Peris, Eur. J. Inorg. Chem. (2003) 1215.
[83] B. Cetinkaya, P.B. Hitchcock, M.F. Lappert, D.B. Shaw, K. Spyropoulos, N.J.W. Warhurst, J. Organomet. Chem. 459 (1993) 311.
[84] M. Alcarazo, S.J. Roseblade, A.R. Cowley, R. Fernandez, J.M. Brown, J.M. Lassaletta, J. Am. Chem. Soc. 127 (2005) 3290.

[85] R.J. Rubio, G.T.S. Andavan, E.B. Bauer, T.K. Hollis, J. Cho, F.S. Tham, B. Donnadieu, J. Organomet. Chem. 690 (2005) 5353.
[86] F. Iwasaki, N. Manabe, M. Yasui, N. Matsumura, N. Kamiya, H. Iwasaki, Bull. Chem. Soc. Jpn. 69 (1996) 2749.
[87] A.A. Danopoulos, A.A.D. Tulloch, S. Winston, G. Eastham, M.B. Hursthouse, Dalton (2003) 1009.
[88] F.E. Hahn, M.C. Jahnke, V. Gomez-Benitez, D. Morales-Morales, T. Pape, Organometallics 24 (2005) 6458.
[89] A.A. Danopoulos, A.A.D. Tulloch, S. Winston, G. Eastham, M.B. Hursthouse, Dalton Trans. (2003) 1009.
[90] S. Grundemann, M. Albrecht, J.A. Loch, J.W. Faller, R.H. Crabtree, Organometallics 20 (2001) 5485.
[91] D.J. Nielsen, A.M. Magill, B.F. Yates, K.J. Cavell, B.W. Skelton, A.H. White, Chem. Commun. (2002) 2500.
[92] J.R. Miecznikowski, S. Grundemann, M. Albrecht, C. Megret, E. Clot, J.W. Faller, O. Eisenstein, R.H. Crabtree, Dalton Trans. (2003) 831.
[93] D.S. McGuinness, N. Saendig, B.F. Yates, K.J. Cavell, J. Am. Chem. Soc. 123 (2001) 4029.
[94] A.A. Danopoulos, N. Tsoureas, J.C. Green, M.B. Hursthouse, Chem. Commun. (2003) 151.
[95] S. Gischig, A. Togni, Eur. J. Inorg. Chem. (2005) 4745.
[96] J.G. de Vries, Dalton (2006) 421.
[97] D. Pugh, A.A. Danopoulos, unpublished work.
[98] A.A. Danopoulos, J.A. Wright, W.B. Motherwell, Chem. Commun. (2005) 784.
[99] F. Iwasaki, H. Nishiyama, M. Yasui, M. Kusamiya, N. Matsumura, Bull. Chem. Soc. Jpn. 70 (1997) 1277.
[100] S. Gischig, A. Togni, Organometallics 23 (2004) 2479.